GEOLOGICAL SURVEY OF CANADA
OPEN FILE 7308

Shallow Crustal Structure in the Meadowbank River - Tehek Lake Area: Insights from Gravity and Magnetic Modelling

M.D. Thomas

A Contribution to the Uranium - Northern Canada Project
Geo-mapping for Energy and Minerals (GEM) Program

2012

Natural Resources Canada | Ressources naturelles Canada

Canada

GEOLOGICAL SURVEY OF CANADA
OPEN FILE 7308

Shallow Crustal Structure in the Meadowbank River - Tehek Lake Area: Insights from Gravity and Magnetic Modelling

M.D. Thomas

A Contribution to the Uranium - Northern Canada Project
Geo-mapping for Energy and Minerals (GEM) Program

2012

doi:10.4095/292157

This publication is available for free download through GEOSCAN (http://geoscan.ess.nrcan.gc.ca/).

Recommended citation
Thomas, M.D., 2012. Shallow crustal structure in the Meadowbank River - Tehek Lake area: Insights from gravity and magnetic modelling; Geological Survey of Canada, Open File 7308, 42 p. doi:10.4095/292157

Publications in this series have not been edited; they are released as submitted by the author.

Table of Contents

	Page
Abstract	i
Introduction	1
Regional Geology	1
Gravity Field in Study Area	1
Magnetic Field in Study Area	7
Physical Rock Properties	10
Magnetic Susceptibilities of Iron Formation	13
Modelling of Regional Gravity Profiles 1 and 2	13
Relationship between Gravity and Geology, Profile 1	13
Gravity Model Profile, 1	14
Relationship between Gravity and Geology, Profile 2	14
Gravity Model Profile, 2	16
Modelling along Detailed Traverses A and B	18
Magnetic Model, Traverse A	18
Gravity Model, Traverse A	25
Magnetic Model, Traverse B	30
Gravity Model, Traverse B	32
Conclusions	34
Acknowledgements	35
References	36
Table 1	12

Abstract

Relatively closely-spaced gravity data measured along two traverses near the Meadowbank gold deposits near Tehek Lake have been modelled in concert with regional magnetic data to provide a preliminary picture of upper crustal structure and rock types. Modelling has also been completed along two regional gravity profiles, indicating that Archean supracrustal rocks attain thicknesses ranging from 2.8 km to 8.3 km in fairly localised keels, but are generally 1000 m to 2000 m thick over large sections of crust. Parts of thinner sections of supracrustal rocks are modelled to be overlain by very thin (<400 m thick) sheets of Archean granitic rocks that may be in intrusive or tectonic contact. Regional modelling also suggests the presence of thin (~3 km thick), buried sheet-like Proterozoic granitic bodies.

Modelling along the detailed gravity traverses yields similar thicknesses of supracrustal rocks, generally between 500 m and 1700 m thick, which are also overlain by thin sheets of Archean granitic rocks. Modelled contacts between supracrustal units are typically very steep. A notable product of magnetic modelling is a large volume of high magnetic susceptibility iron formation distributed in many narrow, steep units extending from the surface or near-surface to depths ranging from about 1000 m to 1200 m. These depths probably represent minimum depths because of limitations in modelling steep, narrow bodies. Another revelation of modelling is the large volumes of komatiite predicted as extensions of relatively small units of komatiite mapped at surface. Granitic bodies of possible Proterozoic age have been modelled in the upper crust. One extends vertically over about 4800 m, whereas others extend no deeper than 1400 m below surface.

Introduction

A relatively detailed (closely spaced measurements) gravity survey has been completed along two traverses in the area of the Meadowbank gold deposits (Sherlock et al., 2004) near Pipedream and Tehek lakes, Nunavut, with a view to investigating deeper aspects of geological structure. Locations of the traverses are shown in Figure 1 superposed on a picture of the regional geological setting presented by Zaleski et al. (2000). Interpretation of gravity profiles along the traverses is preceded by analysis and interpretation of the regional gravity field covering a larger area outlined in Figure 1; the magnetic field in the same area was also analysed. Two-dimensional models have been derived from both the gravity and magnetic data sets.

Geological maps at 1:50 000 scale provide coverage in the central part of the study area straddling longitude 96^{O} between roughly latitudes 64^{O} 30' and 65^{O} 30'. These are identified as Meadowbank R (Zaleski, 2005), Meadowbank R to Tehek Lake (Zaleski et al., 1997), SE Amer Lake (Ashton, 1987), Amarulik Tehek Lakes (Zaleski et al., 2005) and Half Way Hills & Whitehills L (Zaleski and Pehrsson, 2005) on Figure 1. A map at 1:100 000 scale identified as Whitehills Tehek Lakes (Henderson and Henderson, 1994) extends across four of the aforementioned maps. The northwest and northeast quadrants of the study area are covered by 1:250 000 geological maps labelled, respectively, Amer Lake (Tella, 1994) and Woodburn Lake (Fraser, 1987), and the southeast quadrant is covered by a map labelled Baker Lake at 1:125 000 scale produced by Schau (1983). The entire study area is covered by a compilation geological map at a scale of 1: 1 000 000 (Paul et al., 2002). Together these maps provide a robust geological framework for the geophysical studies.

The study commences with an evaluation of relationships between the regional geology and gravity and magnetic fields of the area, and then focuses on modelling of gravity and magnetic anomalies along the two gravity traverses. Rock properties (density and magnetic susceptibility) for 128 rock samples that provide constraints for modelling are also presented and discussed.

Regional Geology

Regional geology of the study area reproduced from Paul et al. (2002) is shown in Figure 2. Archean granitic rocks, granites and granodiorites (Agd) (henceforth termed simply Archean granitic rocks), are present in most parts of the region essentially dominating the geological picture, though occur only as isolated islands within a large area of Archean undifferentiated gneiss (Agn) in the northeast quadrant. The sea of Archean granitic rocks is transected diagonally in the central part of the region by a northeast-trending belt of Archean undifferentiated supracrustal rocks (Ap) that include the Woodburn Lake and Ketyet River groups (Fig. 1) and host the Meadowbank gold deposits. The belt is relatively broad southwest of Tehek Lake, but near the western shore of the lake it is offset to the northwest, narrowing significantly before gradually widening northeastward towards Woodburn Lake. A conspicuous east-northeast-trending belt of metasedimentary rocks of the Amer Group (Pag) (Tella, 1994), surrounded by Archean granitic rocks (Agd), is present in the northwest corner of the area. Other noteworthy elements of the Archean geology are small and generally narrow, linear belts of mafic volcanics and associated sediments (Am), and some belt-like and irregular-shaped areas of orthoquartzite (Aq). A few small scattered units of Proterozoic syenite (Psy) and small to moderate-sized granite units (Pg) are also present. These tend to have a roughly oval shape indicative, perhaps, of a relatively undeformed intrusion.

Gravity Field in Study Area

An area bounded by latitudes 64^{O} 30' and 65^{O} 45', and longitudes 94^{O} 30' and 97^{O} 30' (Fig. 1) is selected to examine the regional context of the gravity field, defined principally by measurements completed as part of Canada's national gravity mapping program. Gravity stations are spaced, on average, about 13 km apart, yielding a relatively low resolution image of the gravity field (Fig. 3) that reflects only larger scale geological elements. The gravity map in Figure 3 is based on values determined on a 3 km grid using the national mapping measurements and the closely spaced measurements along the two gravity traverses near Pipedream Lake.

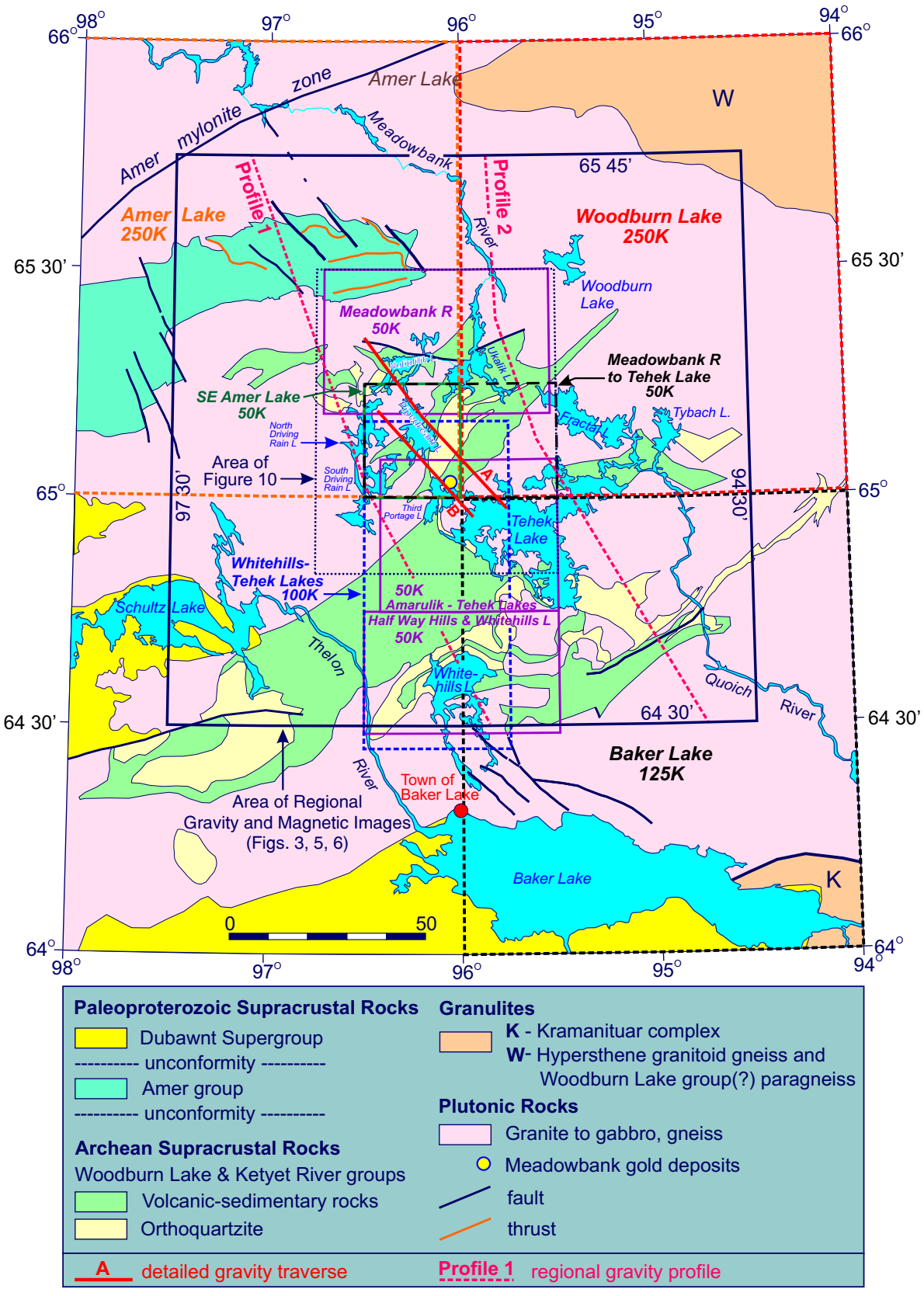

Figure 1: Area of regional gravity study superposed on a simplified regional geological map modified from Zaleski et al. (2000). Locations of detailed gravity traverses, regional gravity profiles and areas of geological mapping are shown. Scale of mapping indicated by an abbreviation, e.g. 250K = 1:250 000 scale. Map areas are identified as: Meadowbank R (Zaleski, 2005), SE Amer Lake (Ashton, 1987), Meadowbank R to Tehek Lake (Zaleski et al., 1997), Amarulik Tehek Lakes (Zaleski et al., 2005), Half Way Hills & Whitehills L (Zaleski and Pehrsson, 2005), Whitehills-Tehek Lakes (Henderson and Henderson, 1994), Amer Lake (Tella, 1994), Woodburn Lake (Fraser, 1987), and Baker Lake (Schau, 1983). The entire study area is covered by a compilation geological map at a scale of 1: 1 000 000 (Paul et al., 2002).

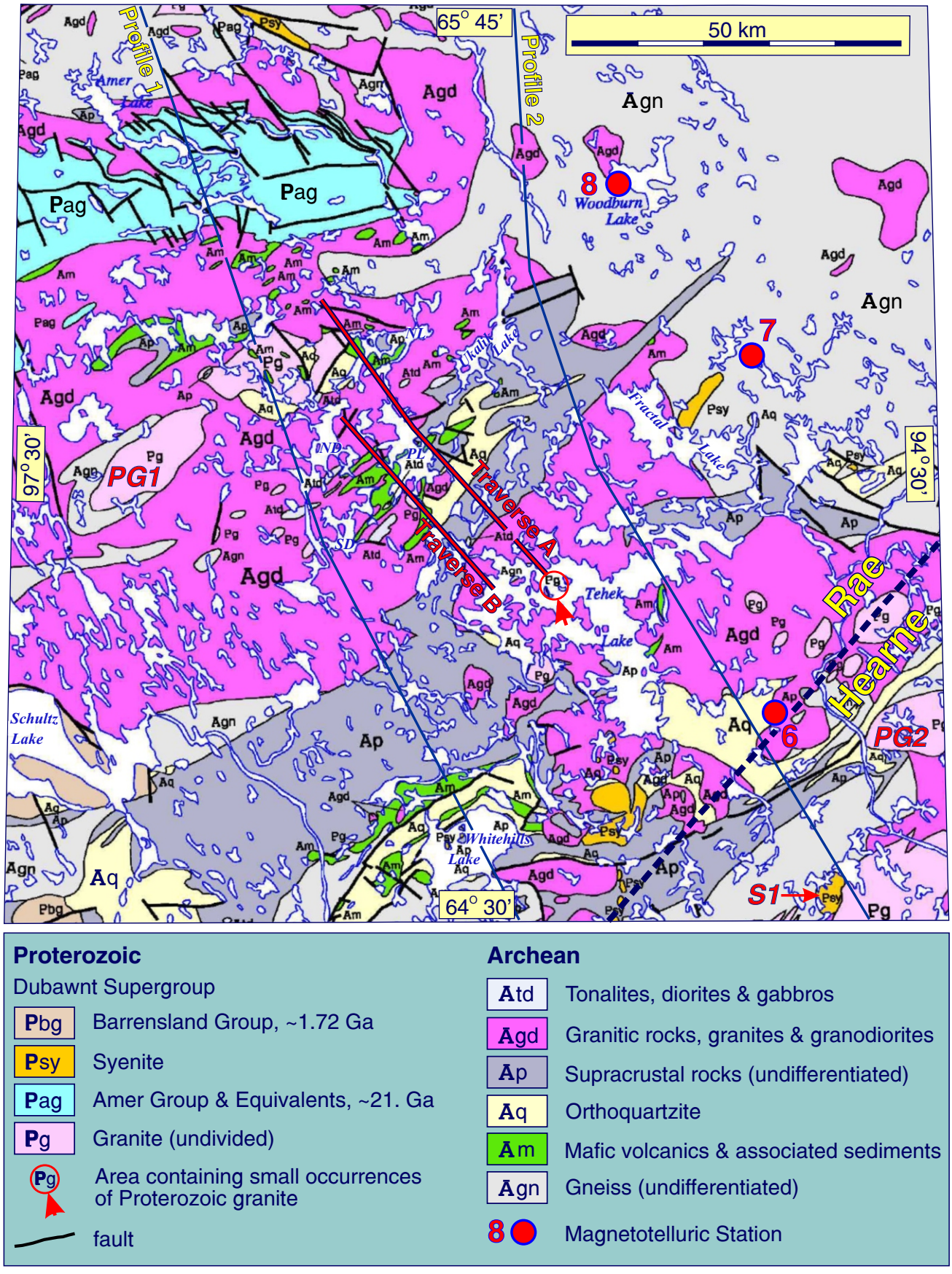

Proterozoic

Dubawnt Supergroup

- Pbg — Barrensland Group, ~1.72 Ga
- Psy — Syenite
- Pag — Amer Group & Equivalents, ~21. Ga
- Pg — Granite (undivided)
- Pg — Area containing small occurrences of Proterozoic granite
- fault

Archean

- Atd — Tonalites, diorites & gabbros
- Agd — Granitic rocks, granites & granodiorites
- Ap — Supracrustal rocks (undifferentiated)
- Aq — Orthoquartzite
- Am — Mafic volcanics & associated sediments
- Agn — Gneiss (undifferentiated)
- 8 — Magnetotelluric Station

Figure 2: Geological map of regional study area reproduced from Paul et al. (2002). PG1 and PG2 (Proterozoic granitic bodies) and S1 (syenite body) are referred to in text. ND, North Driving Rain Lake; NL, Nutiplilik Lake; PL, Pipedream Lake; SD, South Driving Rain Lake. Locations of detailed gravity traverses and regional gravity profiles are shown. Magnetotelluric stations from Jones et al. (2002).

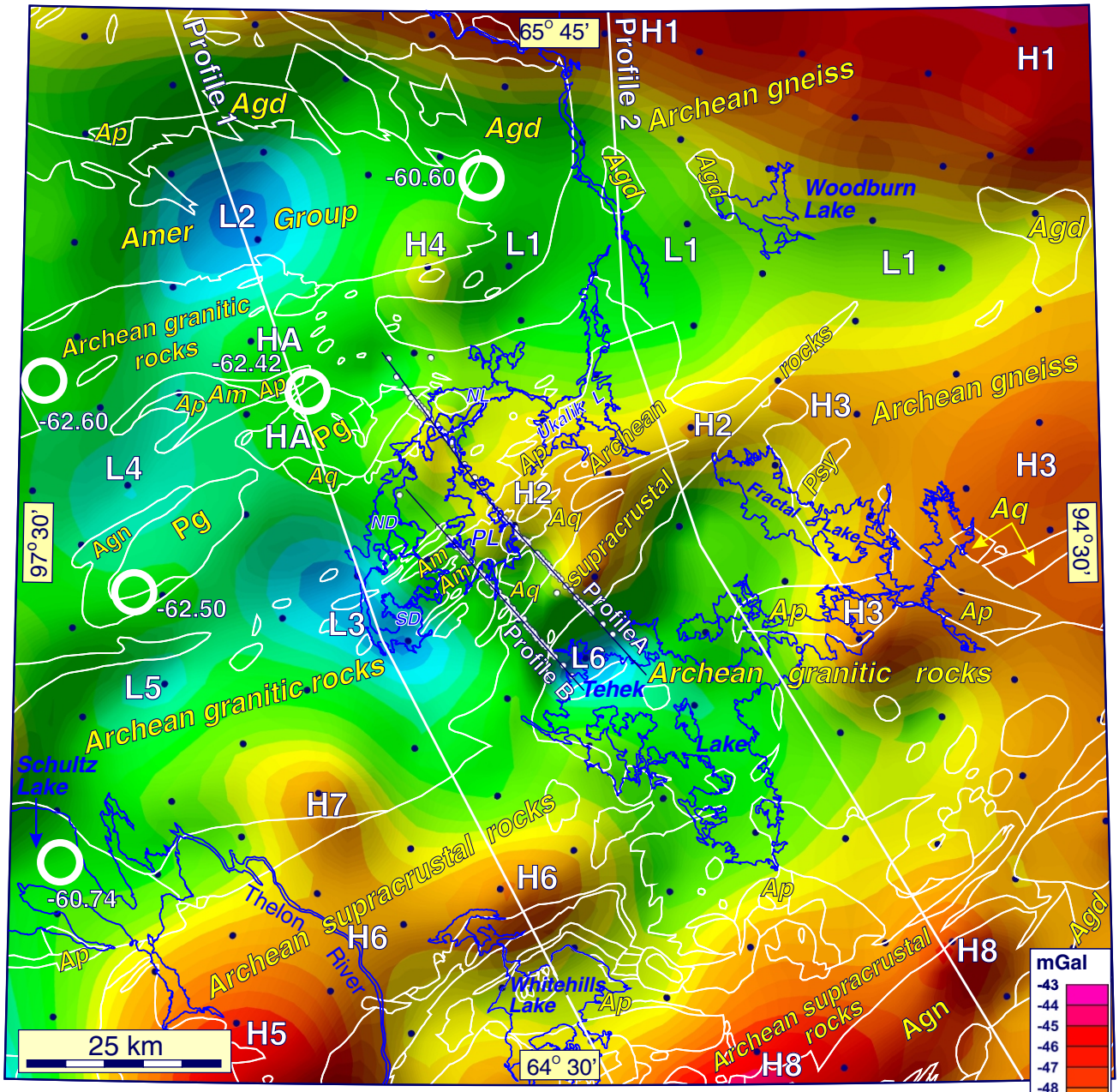

Figure 3: Bouguer gravity anomaly map of regional study area with geological boundaries corresponding to those on Figure 2 superposed. Principal gravity anomalies (highs and lows) are labelled. Locations of paths of two gravity profiles along the detailed gravity traverses and two regional profiles used for modelling are plotted. ND, North Driving Rain Lake; NL, Nutiplilik Lake; PL, Pipedream Lake; SD, South Driving Rain Lake.

These traverses run northwest from the north shore of Tehek Lake, the longer one (~ 46 km long) passing near the northeastern shore of Pipedream Lake, and the shorter one (~26 km long) passing near the southwestern shore. The distribution of gravity stations along the traverses is shown on Figure 3, but is more clearly portrayed on the gravity map of Figure 10, which displays also geological contacts mapped at 1:50 000 scale. Most stations along the traverses are about 300 m to 1000 m apart, yielding gravity profiles providing a measure of detail permitting examination of the finer elements of the geology.

The geological significance of the regional gravity field is examined by comparing it with regional geology defined at a scale of 1:1 000 000 (Fig. 2, after Paul et al., 2002). Reference to other geological maps is made where appropriate. The gravity field (Fig. 3) is characterized by a series of relatively positive (high) and negative (low) anomalies having various spatial dimensions and geometries, amplitudes and orientations, and arranged in no particular pattern. An obvious background level of the field is not apparent, leading to uncertainty in the estimation of amplitudes of anomalies. However, there are several locations where the gravity field may be considered "neutral" with respect to adjacent gravity highs and lows (Fig. 3). Gravity values in these locations range from -62.60 to -60.60 mGal and average -61.77 1.01 mGal, a value adopted as the level of the background gravity field. Amplitudes of anomalies are determined with respect to this value. Comparison of the gravity field and geology is assisted by two long gravity profiles extending north-northeast to south-southwest across the area (Fig. 4a, b).

Bouguer gravity anomalies range from about -43 mGal (gravity high **H1**) near Woodburn Lake in the northeast over Archean undifferentiated gneiss (Agn) (Paul et al., 2002), to about -67.5 mGal in the two most prominent gravity lows, **L2** centred on the mainly metasedimentary Amer Group (Pag) and **L3** coinciding mainly with Archean granitic rocks (Agd). The unit of undifferentiated gneiss (Agn) in the northeast is presumably based on Fraser's (1987) mapping, which also delineated a granulite complex that extends into the northeast corner of the study area. It is speculated that mafic granulitic rocks, possibly at shallow depth below the undifferentiated gneisses, are the source of gravity high **H1**. Such rocks commonly contain relatively high density pyroxene and garnet.

Gravity lows **L2** and **L3** have relatively small amplitudes of about -5.6 and -6 mGal, respectively, and similar spatial dimensions. **L2** is circular and about 30 km in diameter, and **L3** is roughly oval, about 35 km long, and its major axis trends northwest. Another distinct gravity low, **L6**, amplitude about -4.9 mGal, is centred over the northwestern shoreline of Tehek Lake, where it coincides with Archean granitic rocks (Agd). It is a relatively more intense low within a broader low coinciding mainly with Archean granitic rocks that are widespread in the area of the lake. Low **L6** is separated from low **L3** to the northwest by a gravity "ridge" coinciding with undifferentiated Archean supracrustal rocks (Ap) between highs **H2** and **H6**. Two lows near the western margin of the area, **L4** and **L5**, also coinciding largely with Archean granitic rocks (Agd), each have small amplitudes of about -3.3 mGal. They are separated by a minor gravity high correlating partially with a band of Archean gneiss (Agn) curving around the southwestern margin of a unit of Proterozoic granite (Pg). Gravity low **L1** extends eastward from the eastern margin of the Amer Group (Pag) crossing a narrow unit of Archean granitic rocks (Agd) and then mainly a broad expanse of Archean gneiss (Agn). It may be an "apparent" low lying between the high **H1** to the north and composite high **H2**-**H3** to the south.

Archean granitic rocks (Agd) around Tehek Lake are flanked on many sides by Archean supracrustal rocks (Ap) that apparently are the principal source of gravity highs **H2**, **H5**, **H6** and **H8** (Fig. 3). The highs in the area have amplitudes generally significantly larger, in an absolute sense, than those of gravity lows, ranging from +6 to +17.4 mGal. **H4**, amplitude +6 mGal, is an inconspicuous high north of Nutiplilik Lake spanning Archean granitic rocks (Agd) and the Amer Group (Pag). Its likely source, however, is Archean or Proterozoic monzodiorite to monzonitic rocks and pyroxenite mapped within the area of the high (Zaleski, 2005). These rocks, apparently, are represented by a small unit of mafic volcanics and associated sediments (Am) on the map (Fig. 2) of Paul et al. (2002). The high is defined essentially by only a single gravity station, but its viability is supported by the presence of the aforementioned rock types. The highs **H2** (+8.4 mGal), **H6** (+11.2 mGal) and **H8** (+17.4 mGal) display close correlations with mainly Archean supracrustal rocks (Agd) and to a lesser extent with Archean gneiss (Agn). In areas where such rocks fall on relatively negative gravity anomalies or on

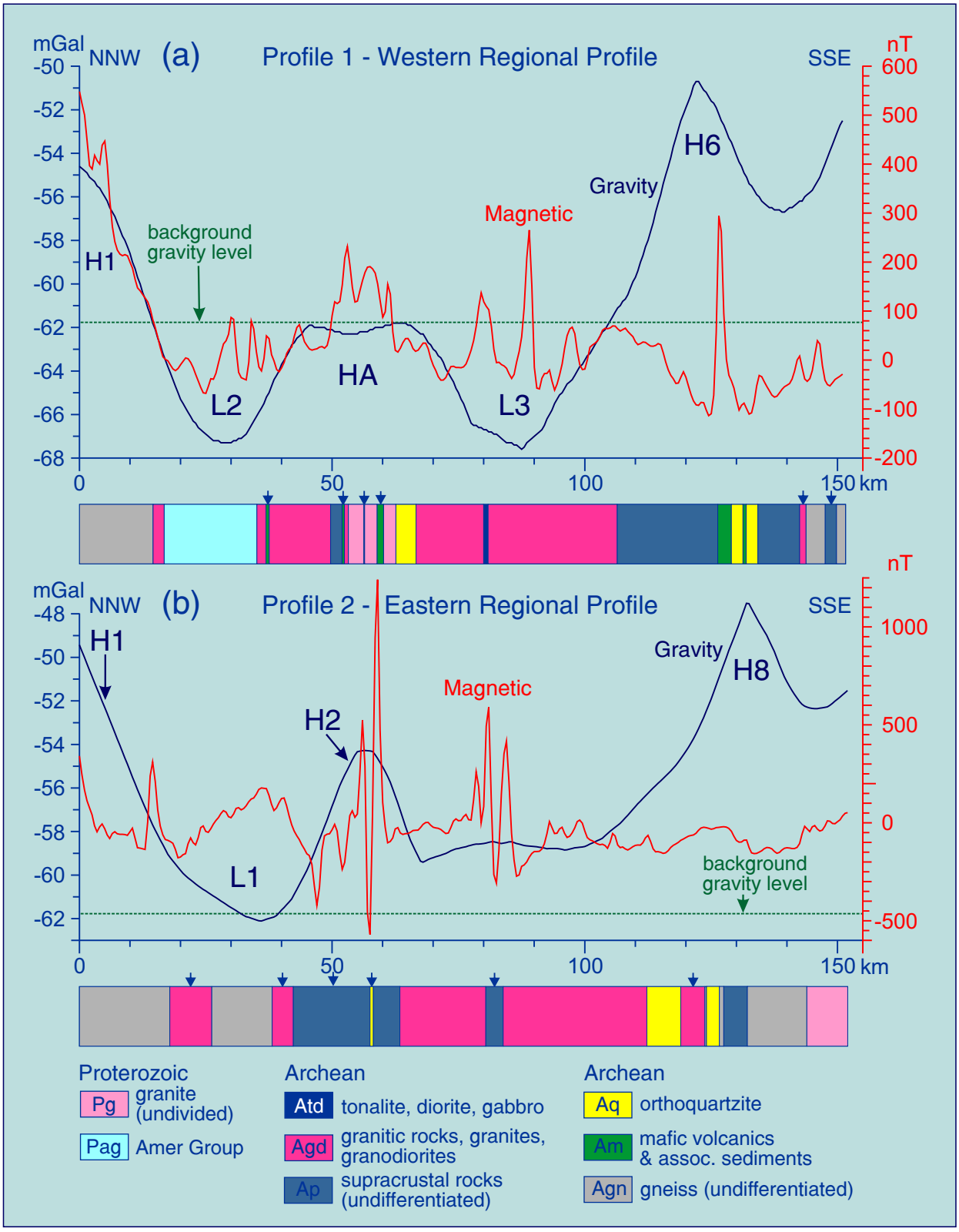

Figure 4: Gravity and total magnetic field profiles and geology along **(a)** Profile **1** (western regional profile) and **(b)** Profile **2** (eastern regional profile). Locations of profiles are shown in Figures 1, 2, 3, 5 and 6. Vertical contacts in the geological sections are schematic; sections simply display the extents of geological units. H, gravity high; L, gravity low. 2D modelling of a profile produces best results when the profile crosses a geological unit near the central point of its strike length. Displacement of the profile from this ideal position results in loss of quality in the model. Geological units probably affected in this manner are identified with an arrow.

gradients they are probably relatively thin or absent. The high **H3** along the eastern margin of the area represents a broadening extension of **H2** and correlates mainly with Archean undifferentiated gneiss (Agn), though small areas of Archean supracrustal rocks (Ap) and orthoquartzite (Aq) are present within its limits. Between **H3** and Wager Bay, east of the area, Archean gneiss contains significant belts of Archean supracrustal rocks. Such supracrustal rocks, as yet unmapped, may be widespread within the area of **H3**.

Magnetic Field in Study Area

Images of the total magnetic field and first vertical derivative of the field are shown in Figure 5 and Figure 6, respectively. The very large range of total magnetic field values in the region, from less than -1000 nT to more than +8800 nT, is consequent on the presence of highly magnetic iron formations. Noticeable in the magnetic images is the strong northeastward trending grain defined by many narrow, parallel to subparallel, linear and curvilinear anomalies. The grain is particularly well developed east of the line of Profile **1** (Figs. 5, 6) over Archean granitic rocks (Agd), Archean gneiss (Agn) and Archean supracrustal rocks (Ap) as portrayed by Paul et al. (2002) (Fig. 2). Particularly strong magnetic anomalies having peak values commonly attaining several thousand nanoteslas present over units of supracrustal rocks are attributed to narrow, interbedded iron formations. In marked contrast, peak values along linear anomalies crossing expanses of Archean granitic rocks (Agd) and gneiss (Agn) are generally less than a couple of hundred nanoteslas.

Strong linear magnetic signatures characterize the east-west belt of Archean supracrustal rocks (Ap) south of Fractal Lake, and the northeast-trending belt between Tehek Lake and Ukalik Lake. The latter belt does not appear southwest of Pipedream Lake (Fig. 2), but strong linear magnetic anomalies, largely coincident with units of Archean mafic volcanics and associated sediments (Am), are present. Detailed geological maps show the presence of iron formations in these units (Ashton, 1987; Zaleski et al., 1997; Zaleski et al., 2005).

A belt of strong magnetic anomalies runs from North Driving Lake northeastward to east-northeastward through Nutiplilik Lake to the northern end of Ukalik Lake. It crosses small areas of Archean supracrustal rocks (Ap), orthoquartzite (Aq) and mafic volcanics and associated sediments (Am) surrounded mainly by Archean granitic rocks (Agd). Narrow developments of iron formation mapped in this area (Zaleski, 2005) are the undoubted source of these anomalies. A strong east-northeast trending linear anomaly (peak value >1850 nT) flanking the southern contact of the Amer Group near its eastern extremity, though coinciding with mainly Archean granitic rocks (Agd) on the map of Paul et al. (2002), is attributed to narrow bands of iron formation and/or Archean or Proterozoic pyroxenite locally containing thin diffuse bands of magnetite mapped by Zaleski (2005).

North and northwest of Whitehills Lake strong linear to curvilinear magnetic highs along the southeastern margin of the widest belt of Archean supracrustal rocks (Ap) in the study area correlate partially with the supracrustal rocks and partially with units of Archean mafic volcanics and associated sediments (Am) (Paul et al., 2002). Peak values are commonly >1000 nT and range up to almost 2500 nT. Mapping by Zaleski and Pehrsson (2005) indicates the presence of iron formation in the anomalous areas. Apart from these marginal anomalies, this broad Archean supracrustal unit is characterized by a relatively featureless magnetic field signifying an absence of iron formation.

West of the line of Profile **1** (Fig. 5) the pattern of magnetic anomalies is irregular and lacks a discernible dominant trend. Conspicuous, however, is a broad region of relatively positive anomaly (total field values range from about 100 to 400 nT) associated mainly with Archean granitic rocks (Agd) located between a Proterozoic granite (PG1 in Figs. 2, 5, 6) and the broad unit of Archean supracrustal rocks (Ap) northwest of Whitehills Lake. The irregular total magnetic field pattern is transected by narrow northwest to north-northwest trending linear lows attributed to faults (Figs. 5, 6). These lows are enhanced in the image of the first vertical derivative (Fig. 6), which defines also distinct narrow linear highs having similar trends. The highs may reflect portions of Archean granitic rocks unaffected by faulting and/or a structural fabric.

A series of narrow, linear magnetic highs, labelled “D” in Figures 5 and 6, in the southwest and northwest quadrants of the area are interpreted to reflect mafic dykes. Two dykes are interpreted in the southwest, one

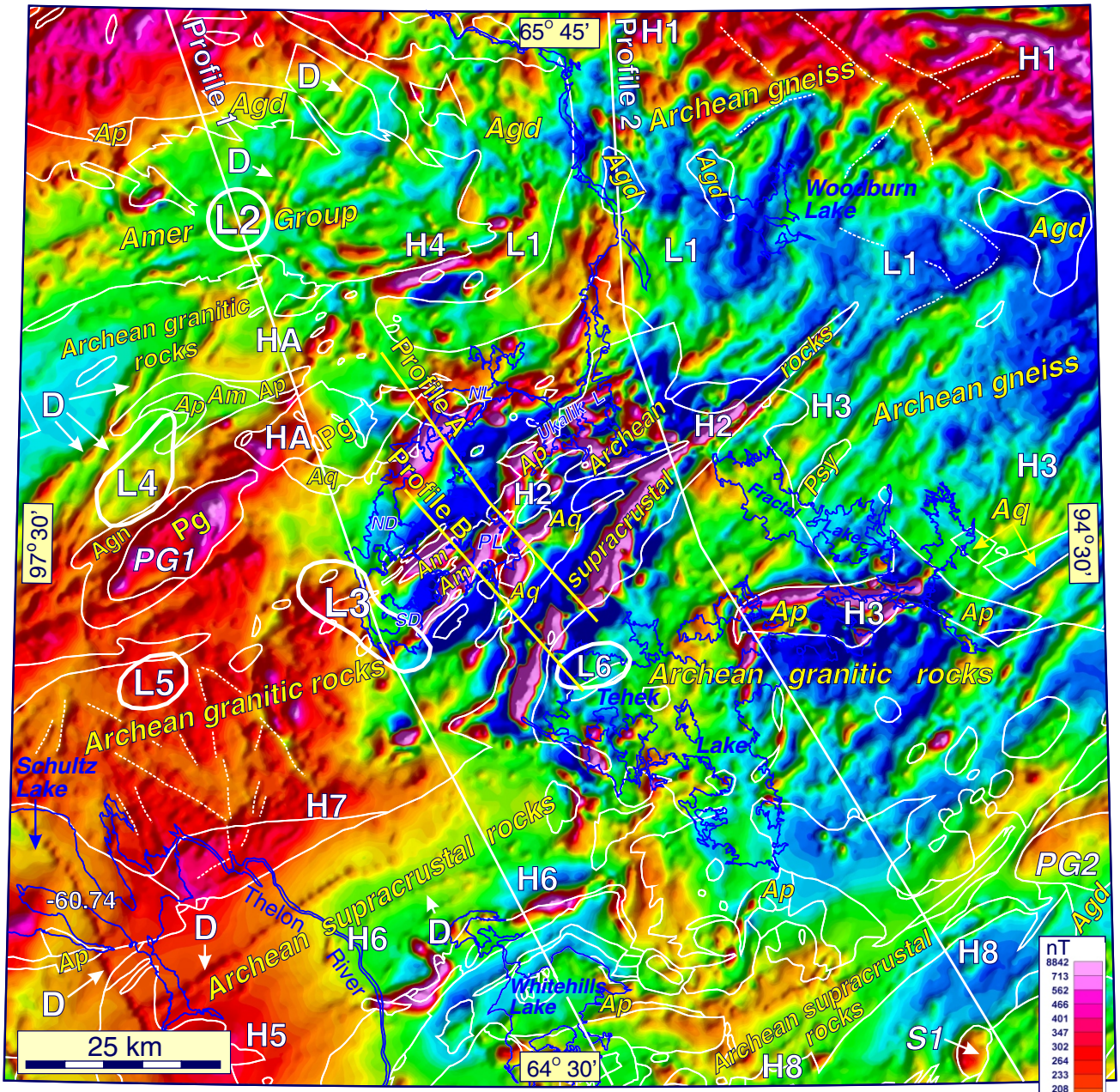

Figure 5: Image of the total magnetic field in the study area with geological boundaries corresponding to those on Figure 2 superposed. Locations of gravity highs and lows labelled in Figure 3 are plotted along with the approximate limits of selected gravity lows. PG1 and PG2 (Proterozoic granitic bodies) and S1 (syenite body) are referred to in text. ND, North Driving Rain Lake; NL, Nutiplilik Lake; PL, Pipedream Lake; SD, South Driving Rain Lake.

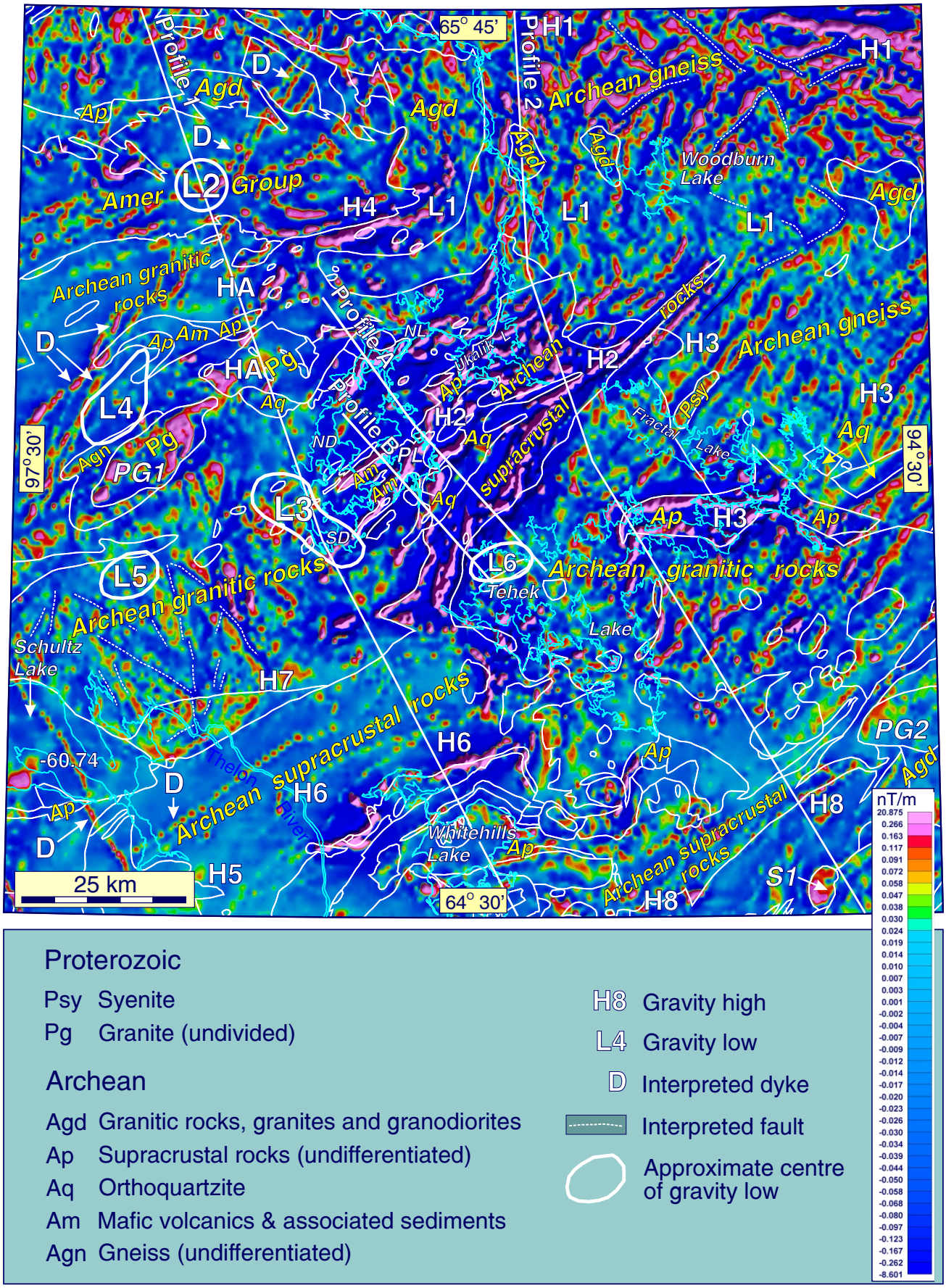

Figure 6: Image of the first vertical derivative of the total magnetic field in the study area with geological boundaries corresponding to those on Figure 2 superposed. Locations of gravity highs and lows labelled in Figure 3 are plotted, along with the approximate limits of selected gravity lows. PG1 and PG2 (Proterozoic granitic bodies) and S1 (syenite body) are referred to in text. ND, North Driving Rain Lake; NL, Nutiplilik Lake; PL, Pipedream Lake; SD, South Driving Rain Lake.

oriented northwest and one northeast. The magnetic highs in the northwest indicate the presence of two sets of dykes, one trending roughly N30^{o}E and the other northeast. An area of moderately strong positive magnetic signature in the northeast corner of the area falling within a broad unit of Archean gneiss (Agn) coincides closely with gravity high H1. It is another indication that the gneiss, locally, is distinct from gneiss elsewhere within the unit. The positive magnetic signature in the northwest corner, though unaccompanied by a gravity high, may also signify a discrete unit of gneiss.

Several Proterozoic granite bodies punctuate the dominantly Archean terrain. They are generally oval to roughly oval in shape, suggestive of the initial form at the time of intrusion. Most are not associated with a distinctive magnetic signature, although the Proterozoic granitic body, PG2 in Figures 2, 5, and 6, displays a weak positive signature over its northern half. In contrast, the Proterozoic granite body, PG1, west of Pipedream Lake has a distinct positive magnetic signature. A few small units of Proterozoic syenite (Psy) are present in the eastern half of the area (Fig. 2), only one of which (S1 in Figs. 2, 5, 6) produces a closely correlative magnetic expression in the form of an oval magnetic high.

Physical Rock Properties

Knowledge of rock densities and magnetic susceptibilities, respectively, provides a key constraint for quantitative modelling of gravity and magnetic anomalies. In this study such knowledge is provided by archived rock property measurements made on 128 roughly hand-size samples collected from the study area. Sample locations are illustrated in Figure 7, which displays also a compilation of the geology based on 1:50,000 scale mapping (Ashton, 1987; Zaleski, 2005; Zaleski and Pehrsson, 2005; Zaleski et al., 1997; Zaleski et al., 2005) as a reference framework. These relatively few rock property determinations provide an indication of the ranges of densities and magnetic susceptibilities for particular rock types within the area. These are listed in Table 1.

Densities of the various igneous rock types are typical of density values recorded for such rock types in many areas of the Canadian Shield. The characteristic increase in density with increasing basicity is observed. For plutonic rocks the mean density of all "granites" (includes Archean and Proterozoic granites, granodiorites and tonalites) is 2.66 g/cm^3, and this value jumps to 2.92 g/cm^3 for diorites and 3.03 g/cm^3 for gabbros. A similar pattern emerges for volcanic equivalents with porphyry and felsic volcanic rocks having low mean densities of 2.67 g/cm^3 and 2.71 g/cm^3, respectively, and more basic intermediate and mafic volcanic rocks yielding mean densities of 2.76 g/cm^3 and 2.89 g/cm^3, respectively. Diabase and mafic dykes have a reasonably characteristic mean density value of 2.86 g/cm^3 and a moderately high mean susceptibility value of 16.16 SI x 10^{-3}.

The mean density for ultramafic rocks is relatively low at 2.87 g/cm^3 suggesting that they have been subject to serpentinization, which characteristically generates magnetite and relatively low density (2.39 g/cm^3) brucite. Evidence for serpentinization is manifested in a relatively high mean magnetic susceptibility of 40.34 SI x 10^{-3}, and a maximum value of 147 SI x 10^{-3} (Table 1). Magnetic susceptibilities for other plutonic rock types are generally quite low (<1 SI x 10^{-3}), though Archean granitic rocks have a mean value >5 SI x 10^{-3}, and diorites have a mean magnetic susceptibility >6 SI x 10^{-3}. Low mean values of susceptibility are observed also for volcanic rock types, the highest value being just 1.03 SI x 10^{-3} for intermediate volcanic rocks.

In the categories of metamorphic and metasedimentary rocks mean densities are considered typical for the various rock types with quartzite yielding a value of 2.66 g/cm^3, and amphibolite, slate and greywacke having values of 2.98 g/cm^3, 2.76 g/cm^3 and 2.74 g/cm^3, respectively. Amphibolite has a moderately high mean magnetic susceptibility value of 11.60 SI x 10^{-3}, and greywacke is slightly magnetic as indicated by a mean susceptibility of 3.47 SI x 10^{-3} (Table 1).

Figure 7 [Next Page]: Locations of rock samples used for measurements of density and magnetic susceptibility. Geology is compiled from 1:50,000 scale geological maps (Ashton, 1987; Zaleski, 2005; Zaleski and Pehrsson, 2005; Zaleski et al. 1997; Zaleski et al., 2005). Names of geological maps along western border of compilation correspond to names in Figure 1 showing coverage of various maps. A selection of geological units is labelled, but for more detailed information individual maps should be consulted. Table 1 is adapted from Zaleski (2005) with minor modifications. ND, North Driving Rain Lake; NL, Nutiplilik Lake; PL, Pipedream Lake; SD, South Driving Rain Lake.

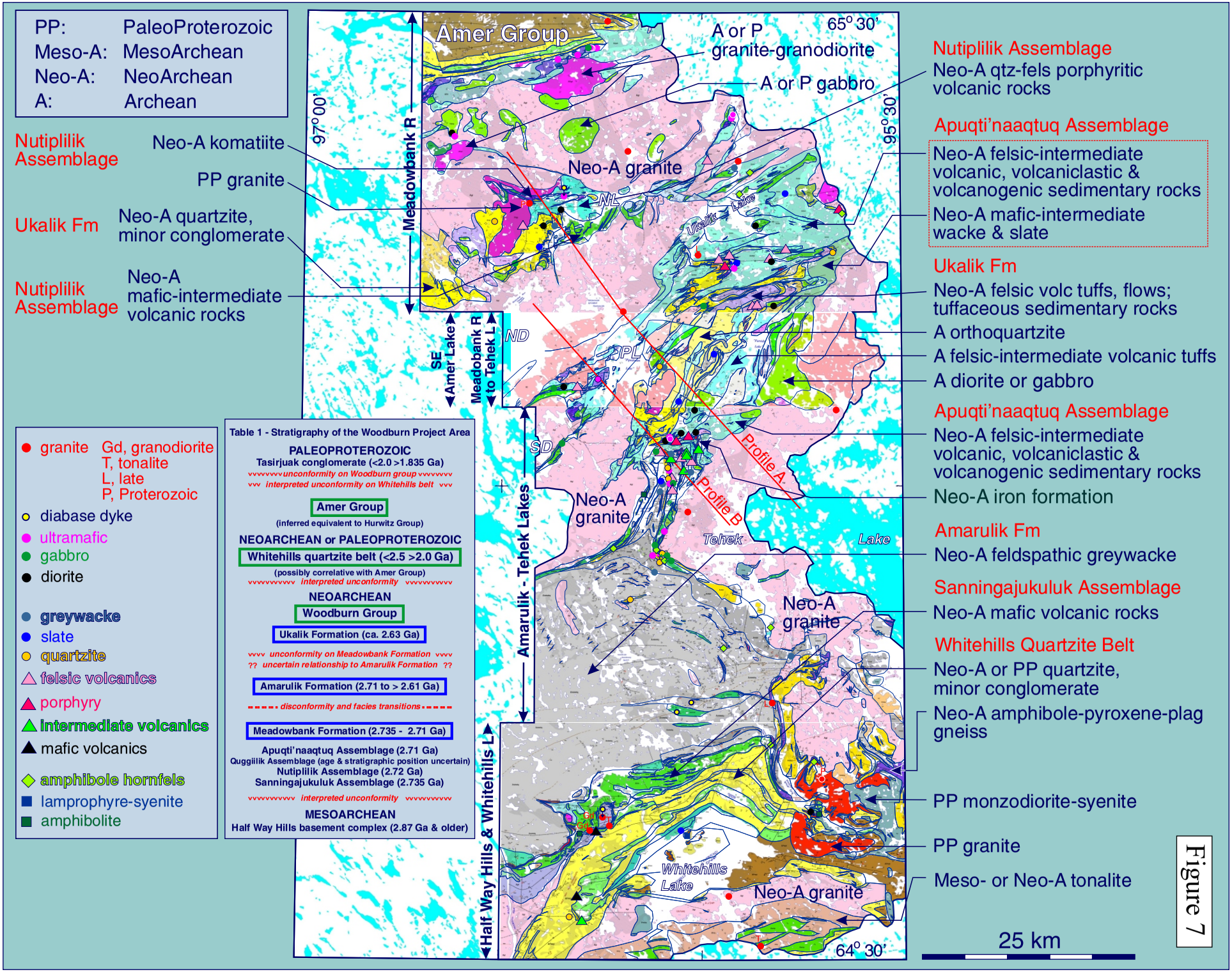
PP: PaleoProterozoic
Meso-A: MesoArchean
Neo-A: NeoArchean
A: Archean
Nutiplilik Assemblage
Neo-A komatiite
PP granite
Ukalik Fm
Neo-A quartzite, minor conglomerate
Nutiplilik Assemblage
Neo-A mafic-intermediate volcanic rocks
granite Gd, granodiorite T, tonalite L, late P, Proterozoic
diabase dyke
ultramafic
gabbro
diorite
greywacke
slate
quartzite
felsic volcanics
porphyry
intermediate volcanics
mafic volcanics
amphibole hornfels
lamprophyre-syenite
amphibolite
Table 1 - Stratigraphy of the Woodburn Project Area
PALEOPROTEROZOIC
Tasirjuak conglomerate (<2.0 >1.835 Ga)
unconformity on Woodburn group
interpreted unconformity on Whitehills belt
Amer Group
(inferred equivalent to Hurwitz Group)
NEOARCHEAN or PALEOPROTEROZOIC
Whitehills quartzite belt (<2.5 >2.0 Ga)
(possibly correlative with Amer Group)
interpreted unconformity
NEOARCHEAN
Woodburn Group
Ukalik Formation (ca. 2.63 Ga)
unconformity on Meadowbank Formation
?? uncertain relationship to Amarulik Formation ??
Amarulik Formation (2.71 to > 2.61 Ga)
disconformity and facies transitions
Meadowbank Formation (2.735 - 2.71 Ga)
Apuqti'naaqtuq Assemblage (2.71 Ga)
Quggilik Assemblage (age & stratigraphic position uncertain)
Nutiplilik Assemblage (2.72 Ga)
Sanningajukuluk Assemblage (2.735 Ga)
interpreted unconformity
MESOARCHEAN
Half Way Hills basement complex (2.87 Ga & older)
Amer Group
A or P granite-granodiorite
A or P gabbro
65° 30'
97° 00'
95° 30'
Meadowbank R
Neo-A granite
NL
Ukalik Lake
SE Amer Lake
Meadowbank R to Tehek L
ND
SPL
SD
Amarulik - Tehek Lakes
Profile A
Profile B
Tehek Lake
Neo-A granite
Neo-A granite
Half Way Hills & Whitehills L
Whitehills Lake
Neo-A granite
64° 30'
25 km
Nutiplilik Assemblage
Neo-A qtz-fels porphyritic volcanic rocks
Apuqti'naaqtuq Assemblage
Neo-A felsic-intermediate volcanic, volcaniclastic & volcanogenic sedimentary rocks
Neo-A mafic-intermediate wacke & slate
Ukalik Fm
Neo-A felsic volc tuffs, flows; tuffaceous sedimentary rocks
A orthoquartzite
A felsic-intermediate volcanic tuffs
A diorite or gabbro
Apuqti'naaqtuq Assemblage
Neo-A felsic-intermediate volcanic, volcaniclastic & volcanogenic sedimentary rocks
Neo-A iron formation
Amarulik Fm
Neo-A feldspathic greywacke
Sanningajukuluk Assemblage
Neo-A mafic volcanic rocks
Whitehills Quartzite Belt
Neo-A or PP quartzite, minor conglomerate
Neo-A amphibole-pyroxene-plag gneiss
PP monzodiorite-syenite
PP granite
Meso- or Neo-A tonalite

Figure 7

Table 1: Rock Densities and Magnetic Susceptibilities

Lithology	No. of Samples	Density (g/cm^3)				Susceptibility (SI x 10^{-3})			
		Min.	Max.	Mean	S.D.	Min.	Max.	Mean	S.D.
Plutonic Rocks									
All "Granites"	14	2.60	2.71	2.66	0.04	0.01	15.50	3.15	5.24
Archean Granites	8	2.61	2.71	2.66	0.04	0.01	15.50	5.31	6.20
Archean Granodiorites	2	2.70	2.70	2.70		0.03	0.61	0.32	
Archean Tonalites	2	2.68	2.70	2.69		0.02	0.10	0.05	
Proterozoic Granites	2	2.60	2.62	2.61		0.02	0.85	0.44	
Lamprophyre-Syenite	1			2.67				0.03	
Diorites	12	2.77	3.03	2.92	0.07	0.13	37.20	6.20	12.80
Gabbros	10	2.95	3.11	3.03	0.06	0.27	3.45	0.82	0.94
Ultramafic Rocks	18	2.64	3.46	2.87	0.19	0.21	147.00	40.34	4.62
Diabase/Mafic Dykes	5	2.81	2.90	2.86	0.04	0.02	62.20	16.16	26.92
Metamorphic Rocks									
Amphibole Hornfels	10	2.76	3.22	2.89	0.14	0.07	1.65	0.43	0.51
Amphibolite	3	2.91	3.02	2.98	0.06	0.13	34.20	11.60	19.58
Volcanic Rocks									
Porphyry	7	2.61	2.70	2.67	0.04	0.02	0.09	0.05	0.03
Felsic Volcanic Rocks	12	2.59	2.81	2.71	0.06	0.00	3.96	0.39	1.12
Intermed. Volc. Rocks	6	2.62	2.85	2.76	0.08	0.02	5.79	1.03	2.33
Mafic Volcanic Rocks	2	2.83	2.95	2.89		0.45	0.58	0.52	
Metasedimentary Rocks									
Quartzite	10	2.60	2.72	2.66	0.04	0.01	10.40	1.12	3.26
Slate	7	2.66	2.96	2.76	0.10	0.00	0.18	0.06	0.06
Greywacke	11	2.67	2.81	2.74	0.05	0.01	26.70	3.47	7.98

The available physical rock property data provide only a guide to the potential densities and magnetic susceptibilities of rock units in the study area. Their number is small and their distribution is widespread with little or no concentration within any geological unit (Fig. 7), thereby denying accurate estimates of mean values for individual units. Nevertheless, the rock property data in Table 1 provide some measure of a constraint for modelling purposes.

Magnetic Susceptibilities of Iron Formation

Information for magnetic susceptibilities of iron formations in the study area is unavailable. Susceptibilities used in modelling are based, therefore, on published values. Symons and Stupavsky (1983) reported average magnetic susceptibility values for Archean banded iron formations in four mines in the Superior province that range from 503 x 10^{-3} SI to 1206 x 10^{-3} SI. These iron formations are magnetite oxide facies ranging in thicknesses from 50 m to 150 m. In the Hamersley Range, Western Australia, Tompkins and Cowan (2001) reported mean bulk susceptibilities of several hundred 10^{-3} x SI for banded iron formation with several formations having susceptibilities >1000 x 10^{-3} SI. These studies indicate that iron formations can have very large magnetic susceptibilities attaining more than 1000 x 10^{-3} SI. There are, of course, many varieties of iron formation and susceptibilities may vary accordingly. The iron formations in the present study comprise interlayered quartz/iron oxide facies and silicate/carbonate facies.

Symons and Stupavsky (1983) derived an "average equation" relating magnetic susceptibility to specific gravity (SG) for iron formations. This has been used to estimate possible values of density for iron formation in the study area. The equation is as follows:

$kIF = (0.092 \times SG)\ 0.25\ g/cm^3$ (cgs units)

Hence $SG = (kIF + 0.25)/0.092\ g/cm^3$

For SI units $SG = (0.0795772 * kIF + 0.25)/0.092\ g/cm^3$

(kIF = magnetic susceptibility of the iron formation; SG = specific gravity)

Measurements on 452 samples of iron formation (Symons and Stupavsky, 1983) yielded a mean specific gravity of $3.36 \pm 0.31\ g/cm^3$.

Modelling of Regional Gravity Profiles 1 and 2

The regional gravity field (Fig. 3) and gravity profiles (Profiles **1** and **2**, Fig. 4) reveal strong positive gravity responses over areas dominated by Archean supracrustal rocks (Ap). The best examples are gravity highs **H6** (Profile **1**) and **H2** (Profile **2**). The high **H8** (Profile **2**) is another good example, though in this case Archean gneiss (Agn) also contributes to the high, which apparently is the primary influence on gravity high **H1**. These correlations are consistent with available density information (Table 1) and with the estimated background gravity field level of 61.77 mGal (Fig. 4).

Relationship between Gravity and Geology, Profile 1

Along Profile **1** (Fig. 4) gravity high **H6** displays good spatial correlation with a section of crust dominated by Archean supracrustal rocks (Ap), and gravity low **L3** coincides with crust dominated by Archean granitic rocks (Agd). The change from **H6** to **L3** intersects the background level near the contact between granitic (Agd) and supracrustal (Ap) units, thereby supporting the estimated background. Based on a density of 2.76 g/cm^3 for slates and 2.74 g/cm^3 for greywackes (Table 1) Archean supracrustal rocks (Ap) have a mean density

of about 2.75 g/cm^3. Archean granitic rocks (Agd) have a mean density of 2.66 g/cm^3. The mean density of Archean granites, granodiorites and tonalites is marginally higher at 2.67 g/cm^3. Because Archean granitoid rocks are widespread in the study area they are considered to represent the composition of the background crust, for which a density of 2.67 g/cm^3 is adopted. Because the low **L3** falls over presumed background Archean granitic rocks (Agd), a buried granitic body having a density less than 2.67 g/cm^3 is interpreted to underlie the low.

Density data on Archean gneisses are unavailable, but the association of gravity high **H1** at the northwest end of Profile **1** with Archean gneisses (Agn) indicates that the gneisses have a relatively high density. The potential presence of a high density granulite complex in the area of **H1** in the northeast corner of the area has already been discussed. The change from **H1** to the adjacent low **L2** occurs close to the southern contact of the Archean gneiss unit (Agn), near the intersection of the profile and estimated regional background field. This is further support for the selected background value. Low **L2** coincides with the metasedimentary Amer Group (Pag), but is not extensive along the strike length of the group (Fig. 3). It will be argued that **L2** is probably related to a granitic intrusion.

An "apparent" high (**HA**) is present between **L2** and **L3**, its broad peak approximately at the level of the background field. It is conjectured that it is related to a block of "background" crust that in the context of the regional gravity field is not anomalous. Rather the crust in the areas of **L2** and **L3** is of anomalously low density. Geological mapping (Fig. 2) indicates that most of the crustal block associated with **HA** is probably formed of Archean granitic rocks (Agd), though narrow developments of Archean supracustal rocks (Ap), Archean orthoquartzite (Aq), Archean mafic volcanics and associated sediments (Am) and Proterozoic granite (Pg) are also mapped.

Gravity Model, Profile 1

A gravity model derived from Profile **1** (Figs. 2, 3) assuming the level of the background gravity field to be -61.77 mGal is shown in Figure 8. Deviations of the field from this level are anomalies of interest related to crustal units whose densities differ from the density of 2.67 g/cm^3 of "neutral" crust associated with the background field. The lows **L2** and **L3** are modelled in terms of granitic bodies having a density of 2.61 g/cm^3, albeit based on only two measurements of density of Proterozoic granite (Table 1). Both are buried within the unit of Archean granitoids (Agd) having a density of 2.67 g/cm^3. The depth of burial is not unique, but needs to be shallow to reproduce the gradients on the flanks of the anomalies. The granitic bodies were modelled as buried because of the absence of a magnetic signature indicative of a body at surface in the areas of the gravity anomalies. The northern body is modelled between depths of about 600 m and 3400 m, and the southern body lies between about 700 m and 3800 m.

At the north end of the profile gravity high **H1,** coinciding mainly with undifferentiated gneiss (Agn), is attributed to a northward-thickening unit of higher density (arbitrarily chosen to be 2.72 g/cm^3) gneiss that attains a depth of about 4200 m at the end of the profile. This modelled gneiss unit probably includes relatively high density granulitic gneiss. At the south end of the profile, in an area dominated by Archean supracrustal rocks (Ap), the high **H6** is explained by a unit of supracrustal rocks locally attaining a depth of about 4600 m. The unit has a density of 2.75 g/cm^3 compatible with mean densities of 2.76 g/m^3 and 2.74 g/cm^3 for slate and greywacke, respectively (Table 1). Relatively narrow units of Archean gneiss (Agn) are included within the modelled supracrustal unit at the south end of the unit. Most very narrow units in the geological section have not been modelled, because their widths are generally much smaller than the spacing of gravity observations defining the gravity field.

Relationship between Gravity and Geology, Profile 2

In Profile **2** good correlations are observed between gravity high **H2** and Archean supracrustal rocks (Ap), and between **H8** and a section of crust dominated by Archean gneiss (Agn), but including narrower units of

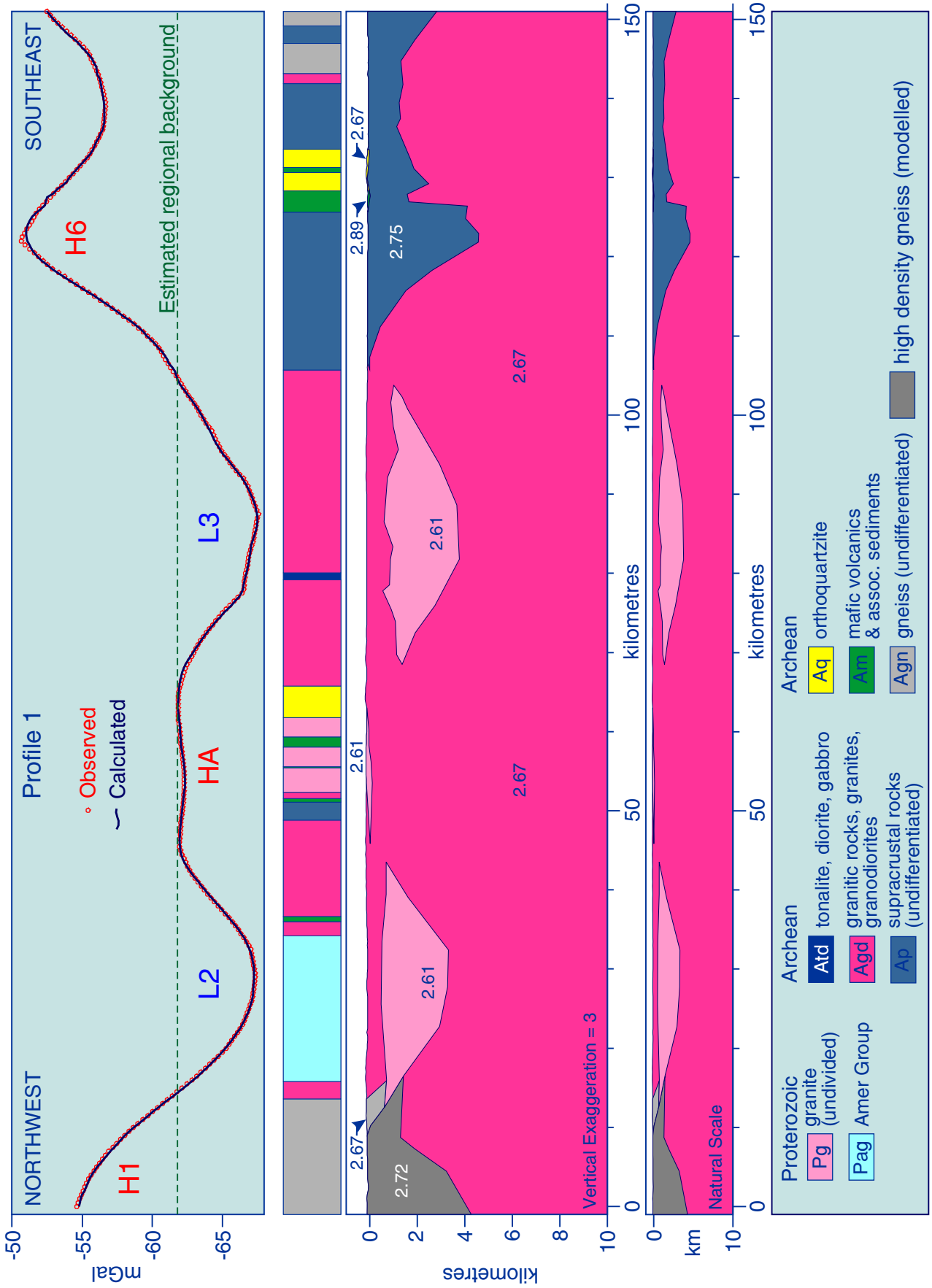

Figure 8: Gravity model derived from Profile **1** (located in Figs. 1, 2, 3, 5, 6); observed and modelled (=calculated) profiles are displayed. Geological section along the path of the profile is also displayed (contacts are schematically portrayed and may or not be vertical). Within the modelled cross section densities of units are indicated in g/cm^3. Gravity highs (H) and lows (L) corresponding to those in Figure 3 are labelled. Modelled crustal section displayed with a vertical exaggeration of 3 and at natural scale.

Archean supracrustal rocks (Ap) and orthoquartzite (Aq) (Fig. 4). The high **H1** at the north end of the profile coincides with undifferentiated Archean gneiss (Agn). The flanking low **L1** to the south also spans a unit of gneiss as well as narrower units of Archean granitic rocks (Agd). Because minimum values within low **L1** are at the same level as the estimated background gravity field, the low is interpreted as an apparent low that like the apparent high (**HA**) between **L2** and **L3** (Profile **1**) is related to a block of "background" crust. Densities of Archean gneisses (Agn) coinciding with **H1** are probably significantly higher than those in the area of **L1**, and as previously argued could be granulitic. The gravity field between **H2** and **H8** is elevated by about 2 mGal with respect to the background field, even though it coincides largely with Archean granitic rocks (Agd). This elevated field might signify that these Archean granitic rocks are relatively high density, or that Archean supracrustal rocks (Ap) or relatively high density Archean gneisses (Agn) underlie Archean granitic rocks.

A clear association between gravity highs and Archean supracrustal rocks is evident, but sources of gravity lows are more problematical. Low **L6** apparently represents a localised "depression" within a significantly broader gravity low correlating with much of a large area of Archean granitic rocks (Agd) surrounding Tehek Lake. It may signify a granitic intrusion, and in fact Paul et al. (2002) show the presence of two very small occurrences of Proterozoic granite on islands within the southeastern margin of the low. If there is a discrete Proterozoic intrusion in this locale it does not generate a magnetic signature (Figs, 5, 6), either because it is not magnetic or because of burial. Peterson (2006) has noted that ~1755 Ma Proterozoic Nueltin granites are leucocratic, contain sparse magnetite and that exposed portions of plutons are associated with a smooth negative magnetic anomaly. A body of Nueltin granite is present little more than 10 km west of the northwest corner of the study area; another is located 95 km south of the southwest corner (Peterson, 2006, Figure 71). Possibly, low **L6** is related to a body of Nueltin granite. This anomaly will be revisited in the section dealing with gravity modelling along the two detailed gravity traverses passing near Pipedream Lake.

Gravity lows **L3**, **L4** and **L5** also fall within a broad expanse of Archean granitic rocks (Agd) and like **L6** are not associated with a magnetic signature. They are defined by very few stations, a possible contributing factor to their smooth circular to oval shape, which is the critical factor in speculating that their sources are granitic intrusions. The amplitudes of **L4** and **L5** are relatively small, just -3.3 mGal, suggesting that any causative intrusion would be thin.

Gravity Model, Profile 2

Gravity high **H1** at the north end of Profile **2** is modelled as a northward-thickening wedge of gneiss that probably contains granulitic components. It has a density of 2.72 g/cm^3 and attains a thickness of about 7.5 km at the end of the profile (Fig. 9). The coincidence of highs **H2** and **H8** with supracrustal rocks (Ap) indicates clearly that the highs are related to such rocks. More problematic is determination of the source of the higher level of the gravity field between these two highs over terrain mapped mainly as Archean granites (Agd) (Fig. 2). This part of the profile is consistently about 3 mGal higher than the estimated regional background. Clues to a possible source are a band of Archean supracrustal rocks (Ap) intersecting the profile between Tehek Lake and Fractal Lake (Fig. 2) and small enclaves of Archean mafic volcanics and associated sediments (Am) lying near the eastern shore of Tehek Lake. Could the band and enclaves be "rooted" in a more continuous layer of Archean supracrustal rocks at depth? If they are, then the exposed Archean granitic rocks likely form a veneer above an extensive supracrustal layer. Modelling completed with this concept in mind outlined a block of supracrustal rocks locally thickened to about 2.8 km and 8.2 km beneath **H2** and **H8**, respectively, and generally about 1 thick between the highs (Fig. 9).

The model poses questions about the nature of the contact between the supracrustal rocks and overlying veneer of Archean granitic rocks. In the central part of the regional study area (Fig. 1) Archean granitic rocks are dated at 2620 - 2600 Ma (Zaleski, 2005; Zaleski et al., 2005). They are younger than the supracrustal Woodburn Group (represented mainly by unit Ap on the 1:1,000,000 scale map of Paul et al. (2002)) which has yielded ages ranging from 2735 2630 Ma (e.g. Zaleski et al., 2005). Zaleski (2005), Zaleski and Pehrsson (2005) and Zaleski et al. (2005) note that Archean supracrustal rocks are enclosed by a voluminous suite of

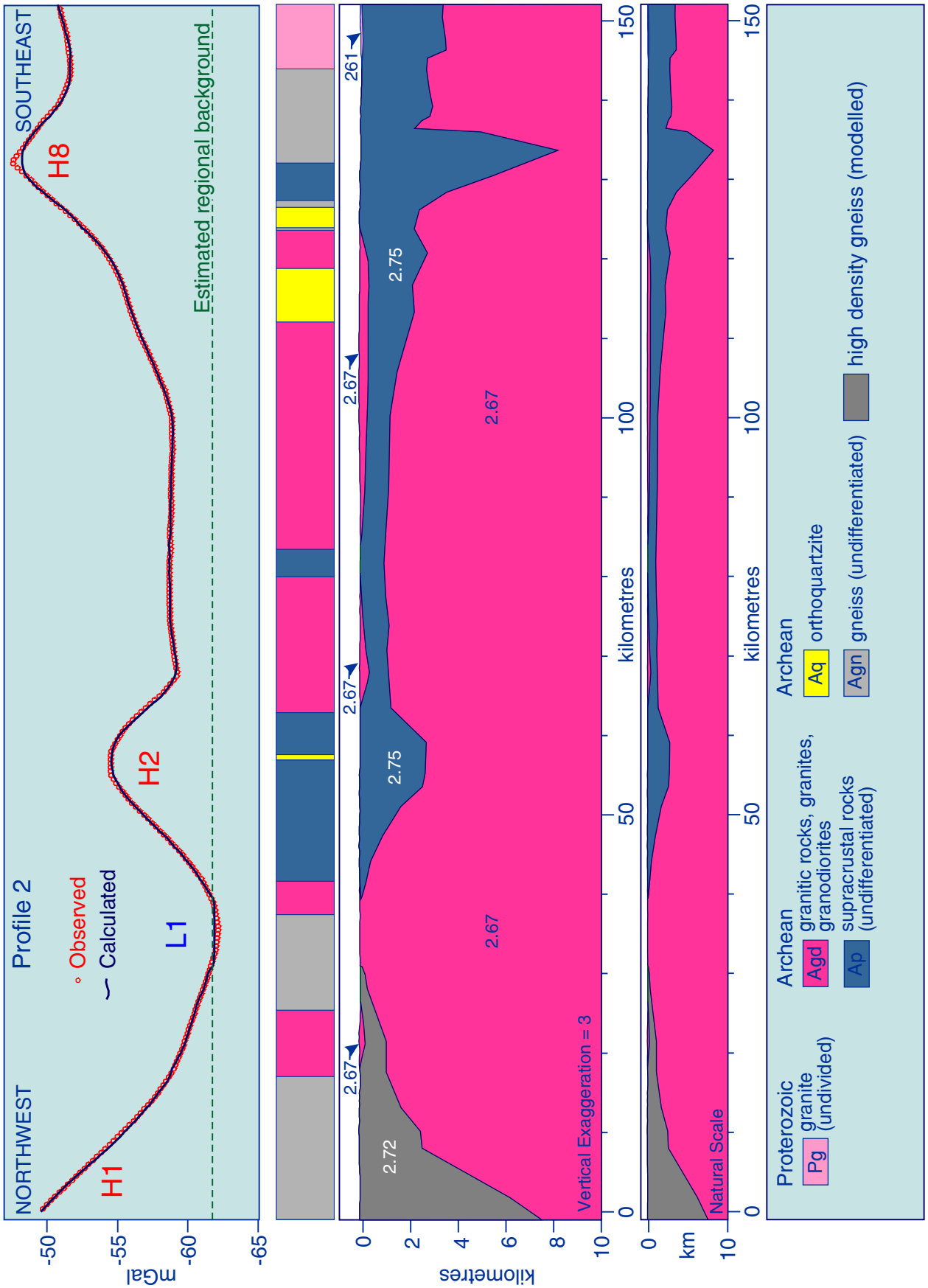

Figure 9: Gravity model derived from Profile **2** (located in Figs. 1, 2, 3, 5, 6); observed and modelled (=calculated) profiles are displayed. Geological section along the path of the profile is also displayed (contacts are schematically portrayed and may or not be vertical). Within the modelled cross section densities of units are indicated in g/cm^3. Gravity highs (H) and lows (L) corresponding to those in Figure 3 are labelled. Modelled crustal section displayed with a vertical exaggeration of 3 and at natural scale.

2620 - 2600 Ma granite, and that intrusive relationships are observed locally. An intrusive relationship between Archean granitic and supracrustal rocks is not inconsistent with the thin skin of Archean granitic rocks portrayed in the model (Fig. 9), an implication being that granitic rocks were intruded as thin sheets.

The picture of a relatively smooth and horizontal contact between a thin sheet of granite and underlying supracrustal rocks seemingly conflicts with the structural history of the region where four main phases of ductile deformation with resultant folding have been recognized. For example, Zaleski et al. (2005) observed mesoscopic intrafolial and isoclinal F1 folds in iron formation and wacke, and Ashton (1988) and Zaleski et al. (2005) noted D2 northwest-verging folds at all scales associated with faults on high-strain fold limbs. D2 reverse faults have also been identified, one such fault forming part of a contact between granite and underlying supracrustal rocks southeast of Pipedream Lake (Zaleski et al., 2005 attributed to Ashton, 1988). The folding aspect of the structural history does question the smoothness of the modelled granite sheets. However, the attitude of the sheets could be influenced by another facet of structure, low angle discontinuities. Several small granite outliers are apparently in low-angle fault contact with underlying ultramafic rocks southwest of Pipedream Lake near Steady Bay (Zaleski et al., 1997) along a narrow (metre-scale) tectonic schist zone dipping ~15^{o} southeast and discordant to regional trends of penetrative fabrics. Syn-D2 low-angle reverse faults are reported in the Half Way Hills and Whitehills Lake map-area (Zaleski and Perhsson, 2005). The bottoms of the granite sheets in the model (Fig. 9) could, therefore, be in the form of a low angle structural discontinuity.

If Archean supracrustal rocks are not present at depth between gravity highs **H2** and **H8** the higher level of gravity field in this area might signify an increase in density of the near-surface crust.

Modelling along Detailed Gravity Traverses A and B

The locations of the two detailed gravity traverses (**A**, **B**) are plotted on the regional maps of geology (Fig. 2), gravity (Fig. 3), total magnetic field (Fig. 5) and first vertical derivative of the magnetic field (Fig. 6), and on the more localized gravity map (Fig. 10) displaying also positions of gravity stations. The profiles are subparallel, oriented approximately northwest-southeast, roughly 7100 m to 8000 m apart and pass along the northeastern and southwestern shores of Pipedream Lake.

Gravity modelling of the traverse profiles was the initial objective of the study. However, the facts that very strong positive magnetic anomalies (amplitudes of 665 nT 3300 nT) clearly related to iron formations correlate with most short wavelength gravity highs (Figs. 11, 12; see Figure 13 for geological legend for these figures), and that density contrasts between units of supracrustal rock units are generally small, dictated that magnetic modelling precede gravity modelling with a view to outlining iron formations. The latter should have high densities, and it was important to see what contribution they made to the gravity field.

Magnetic modelling in this study, in the absence of comprehensive magnetic rock property data, assumes that all magnetization within bodies is induced. It is acknowledged that anisotropy of magnetic susceptibility and natural remanent magnetization are likely present, and that these factors could significantly influence the magnetic signature of an iron formation. Another factor is demagnetization, which can be significant in materials having high magnetic susceptibilities. Magnetic models (Figs. 14, 17) have been derived using the following values for magnetic field parameters: inclination, 86.4^{o}, declination, 4.87^{o}, total magnetic intensity, 60790 nT $\approx$ 48.39 A/m.

Magnetic Model, Traverse A

The prominent magnetic anomalies **m1**, **m2**, **m3**, and **m4** require bodies having very large magnetic susceptibilities to reproduce them, but they correlate mainly with supracrustal rocks that generally have very small magnetic susceptibilities (Table 1). Consequently, units of iron formation possessing large susceptibilities are modelled to explain them. Another outcome of modelling is a need to increase the magnetic susceptibility of sections of upper crust (down to 5 km below sea level) relative to the susceptibility (= zero) of

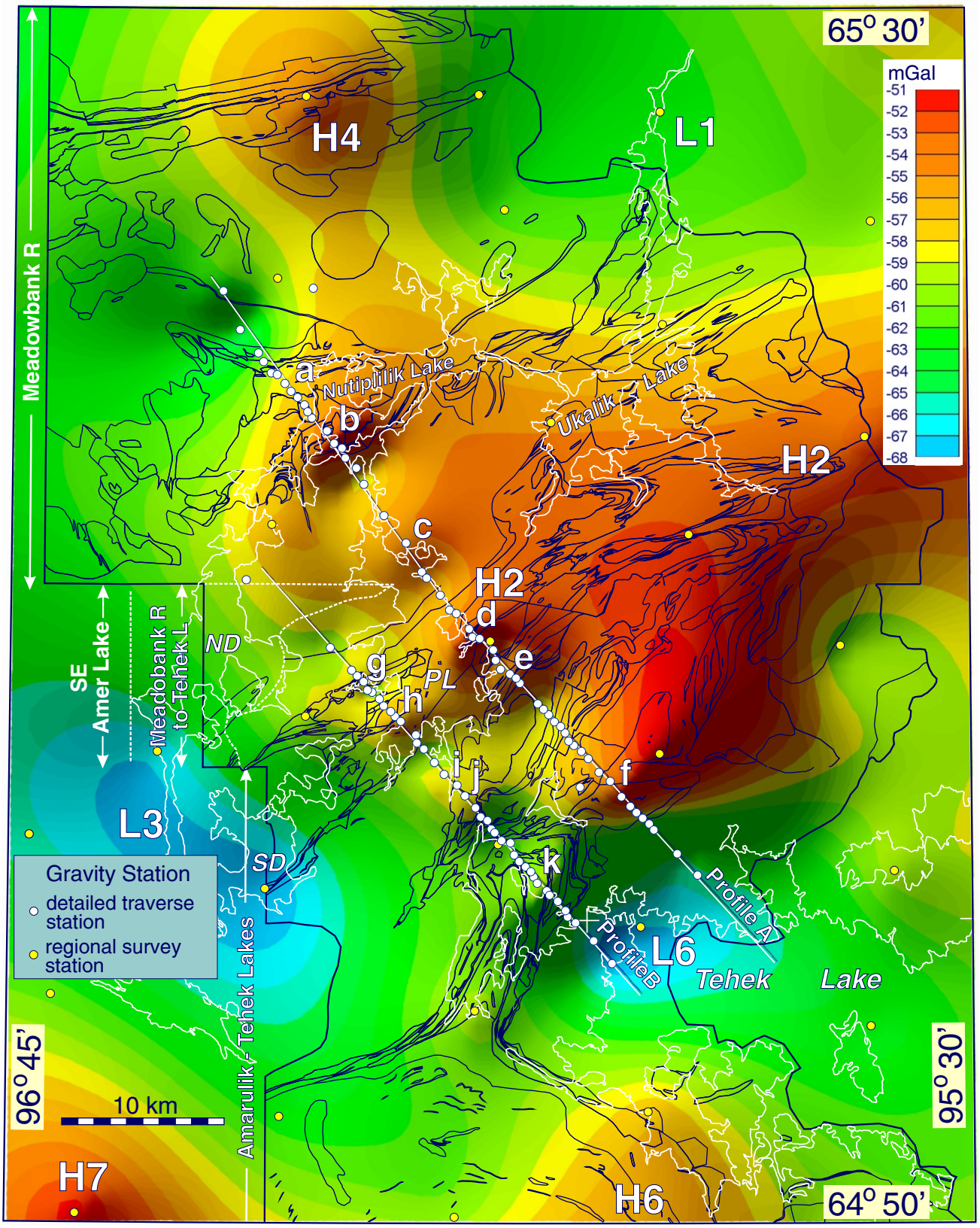

Figure 10: Bouguer gravity anomaly map of the immediate area around the two detailed gravity traverses **A** and **B** based on a grid cell size of 1000 m. Locations of profile lines used for modelling are indicated. Geological boundaries corresponding to those on the 1:50 000 scale maps of the Meadowbank River area (Zaleski, 2005), the "Meadowbank River to Tehek Lake" area (Zaleski et al., 1997), the southeastern Amer Lake area (Ashton, 1987) and the Amarulik and Tehek lakes area (Zaleski et al., 2005) are superposed. Gravity highs and lows in the area corresponding to those on Figure 3 are indicated by H an L accompanied by the appropriate number. PL, Pipedream Lake; ND, North Driving Rain Lake; SD, South Driving Rain Lake.

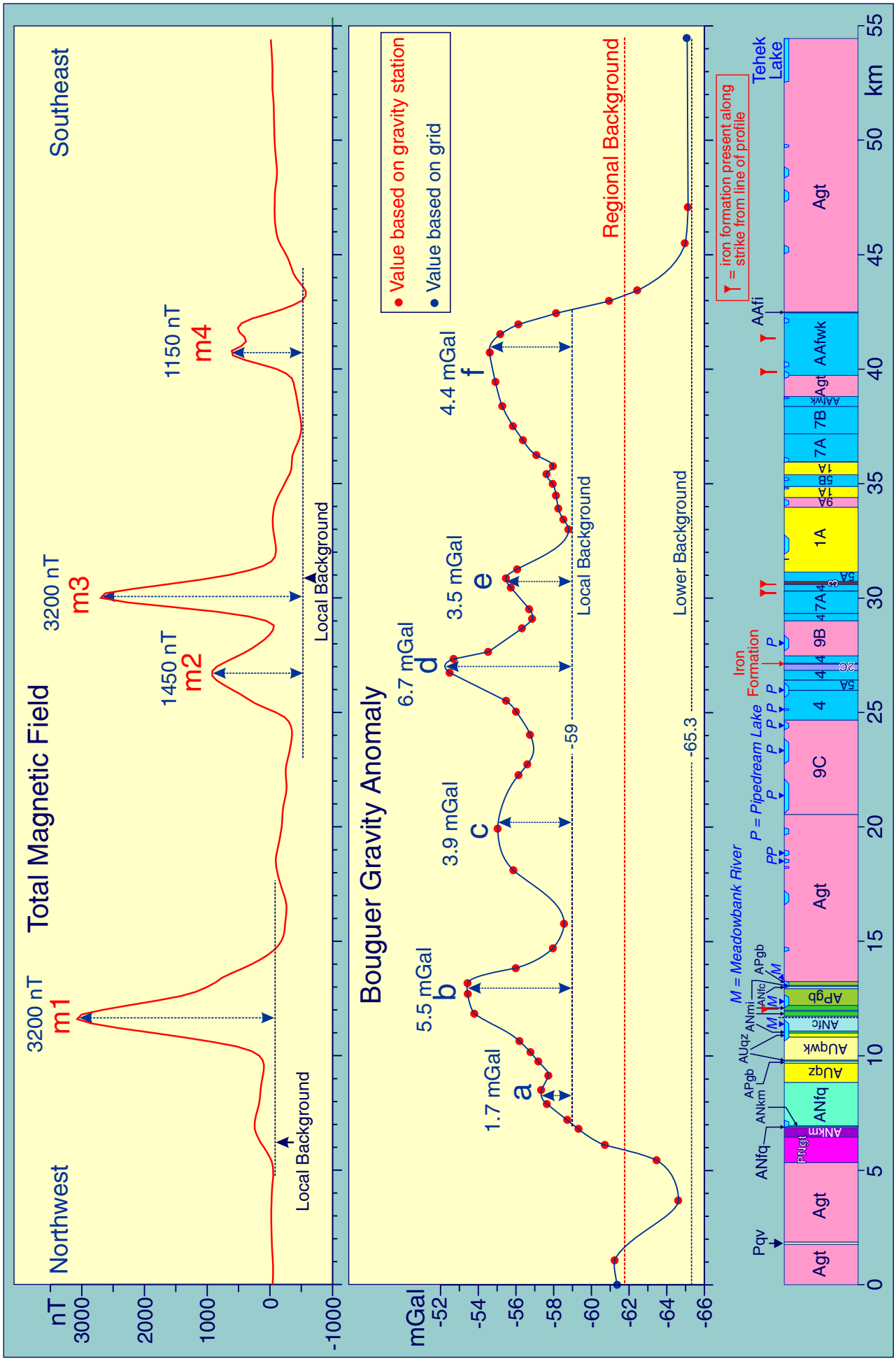

Figure 11: Total magnetic field and Bouguer gravity anomaly profiles and schematic geological section along Traverse **A** (see Figure 13 for legend for geological section). Amplitudes of labeled magnetic and gravity highs are relative to estimated local background levels are indicated.

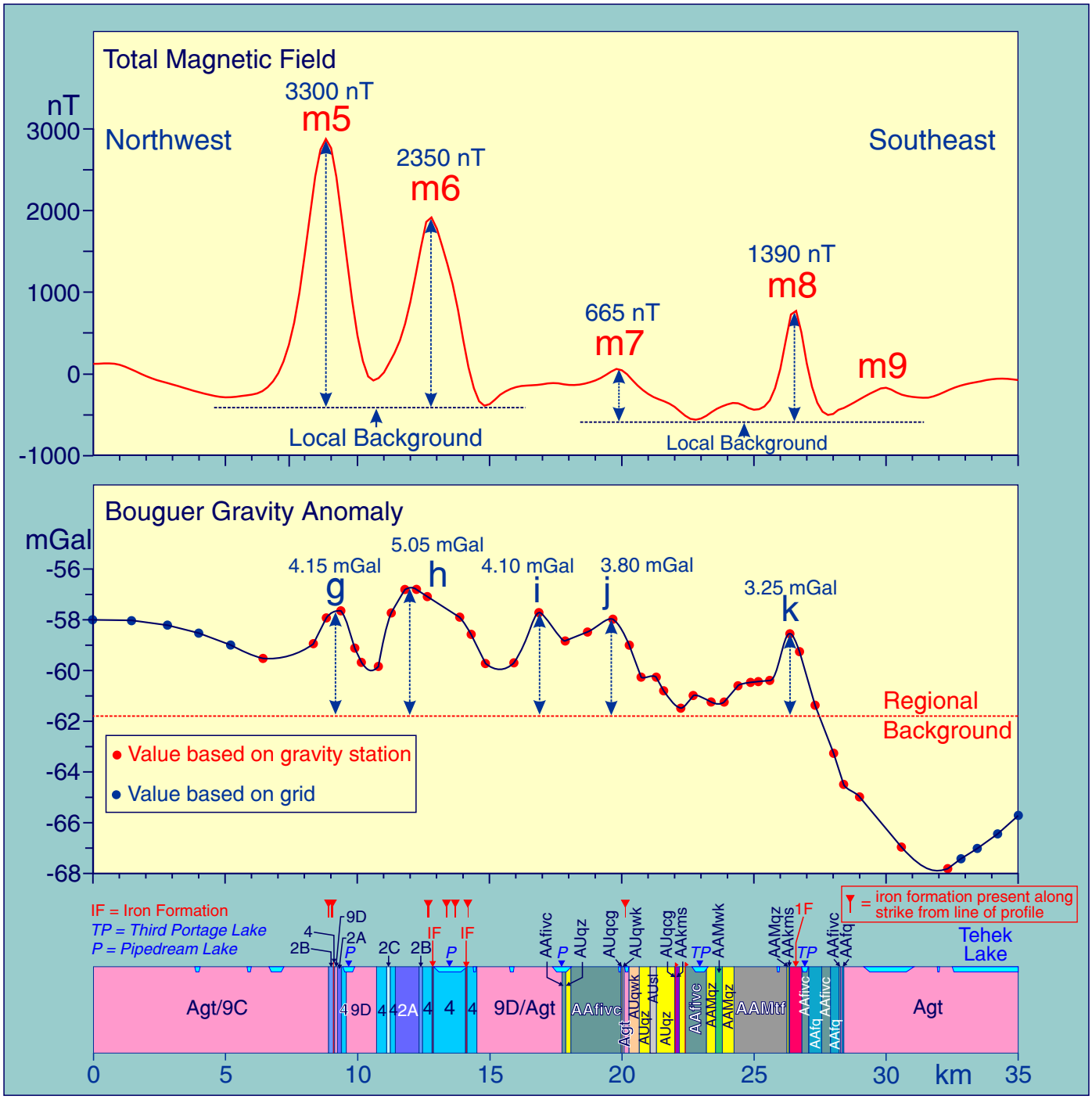

Figure 12: Total magnetic field and Bouguer gravity anomaly profiles and schematic geological section along Traverse **B** (see Figure 13 for legend for geological section). Amplitudes of labeled magnetic and gravity highs are relative to estimated local background levels are indicated.

the Upper Crustal Block 'Central' (Fig. 14) in the area where the fundamental background level of the profile is selected. Adjacent blocks to the north and south have modelled susceptibilities of 22 x 10^{-3} and 4 x 10^{-3}, respectively. These are considered reasonable values for Precambrian crust. For example, Goodge and Finn (2010) modelled 12 km to 15 km thick upper crustal blocks in the East Antarctic Shield having values ranging from 8 x 10^{-3} SI to 71 x 10^{-3} SI. This aspect of the model helps curve-matching of observed and modelled profiles between the large highs.

Many iron formations are modelled to explain each of the magnetic highs, even though iron formation is crossed at only one point by the traverse. They are steep, narrow bodies whose bottoms lie at a constant depth of

1000 m below sea level, generally about 1100 m below the surface. Increasing the depth of the bottom of narrow, steep bodies beyond a certain depth has negligible effect on their magnetic signature. Hence the bottoms are somewhat arbitrarily terminated, and actual depths could be greater. Widths of the modelled iron formations were kept narrow in keeping with widths of mapped units in the study area. A sample of 24 mapped iron formations yielded maximum widths ranging from about 50 m to 380 m, and a mean width of 155 88 m. Widths of modelled iron formations range from about 50 m to 500 m.

Susceptibilities of modelled iron formations have a significant range. For anomaly **m1** the more strongly magnetized bodies have susceptibilities ranging from 80 x 10^{-3} SI to 954 x 10^{-3} SI, while those having weaker magnetizations have susceptibilities ranging from 23 x 10^{-3} SI to 58 x 10^{-3} SI. Possibly some of the latter bodies do not represent iron formation. For **m2** susceptibilities range from 115 x 10^{-3} SI to 220 x 10^{-3} SI, for **m3** the range is 150 x 10^{-3} SI to 660 x 10^{-3} SI, and for **m4** the range is 80 x 10^{-3} SI to 330 x 10^{-3} SI.

Many of the modelled iron formations that collectively reproduce the magnetic high **m1** reach surface. Some lie within unit ANfc which comprises cherty felsic tuffs with iron formation interbeds, and some within unit ANmi comprising mafic-intermediate volcanic rocks. The presence of unmapped iron formations within such units is conceivable. The upper surfaces of some iron formations are terminated by the gabbro unit APgb, which clearly cuts across supracrustal rocks including a unit of iron formation (Zaleski, 2005). Some iron formations are modelled as capped by a thin unit representing the mainly quartzite units AUqz and AUqwk near the northern extremity of **m1**. This modelled unconformable relationship is consistent with the unconformable relationship between the Ukalik Formation and Meadowbank Formation. In some areas iron formation is mapped within quartzites of the Ukalik Formation, hence inclusion of iron formations within a thicker sequence of quartzites is not precluded.

Several steep units of high susceptibility iron formation have been modelled under the lower part of the southern flank of **m1**, their upper surfaces terminated by the lower contact of a granite mapped at surface. This granite is modelled as a thin surface layer, and like thin surficial granite sheets in the regional gravity model along Profile **2** (Fig. 9) is interpreted to be underlain by supracrustal rocks.

Iron formations modelled to satisfy magnetic high **m2** form a steep antiformal pattern. Some are capped by a thin body of granite, whereas others reach surface mainly within felsic-intermediate volcanic tuffs (unit 4, Fig. 14) or tuffaceous volcanic metasedimentary rocks (unit 5A). Both units host iron formations elsewhere in the study area and a single iron formation is mapped at surface. Some iron formations modelled to reproduce the high **m3** reach the surface within the same units and also within unit 7A comprising various tuffs that also host iron formations.

Magnetic high **m4** is also explained by a series of steep, narrow iron formations attaining surface within a unit of felsic-intermediate volcaniclastic rocks and volcanogenic wacke (AAfwk) that hosts iron formation.

The large volume and number of iron formations required to reproduce the principal magnetic highs is surprising, given that iron formation is lacking along the traverse. The perceived absence may be related to extensive overburden cover that has precluded mapping of these very narrow bodies. While the model is not unique, the steep attitudes of these highly magnetic bodies, apparently, are requisite.

Figure 13 [Next Page]: Schematic geological sections along gravity traverses **A** and **B** based on geology on three 1:50 000 scale maps crossed by the traverses. From northwest to southeast these cover the Meadowbank River area (Zaleski, 2005), an area extending between Meadowbank River and Tehek Lake (Zaleski et al., 1997) and the Amarulik and Tehek lakes area (Zaleski et al., 2005). Geological contacts are schematically shown as vertical, the sections portraying only the horizontal width of the geological units at surface. Unit labels as present on the various maps are appended. The legend attempts to correlate units on the Meadowbank River to Tehek Lake map with units within the Meadowbank River area and Amarulik and Tehek lakes area by observing correspondence between units in areas of overlapping coverage. Some units correlate with more than one unit, and hence a need for caution in attribution of units on the Meadowbank River to Tehek Lake map. Correlated units within the latter two areas not present in the sections are enclosed within a red dashed-line box.

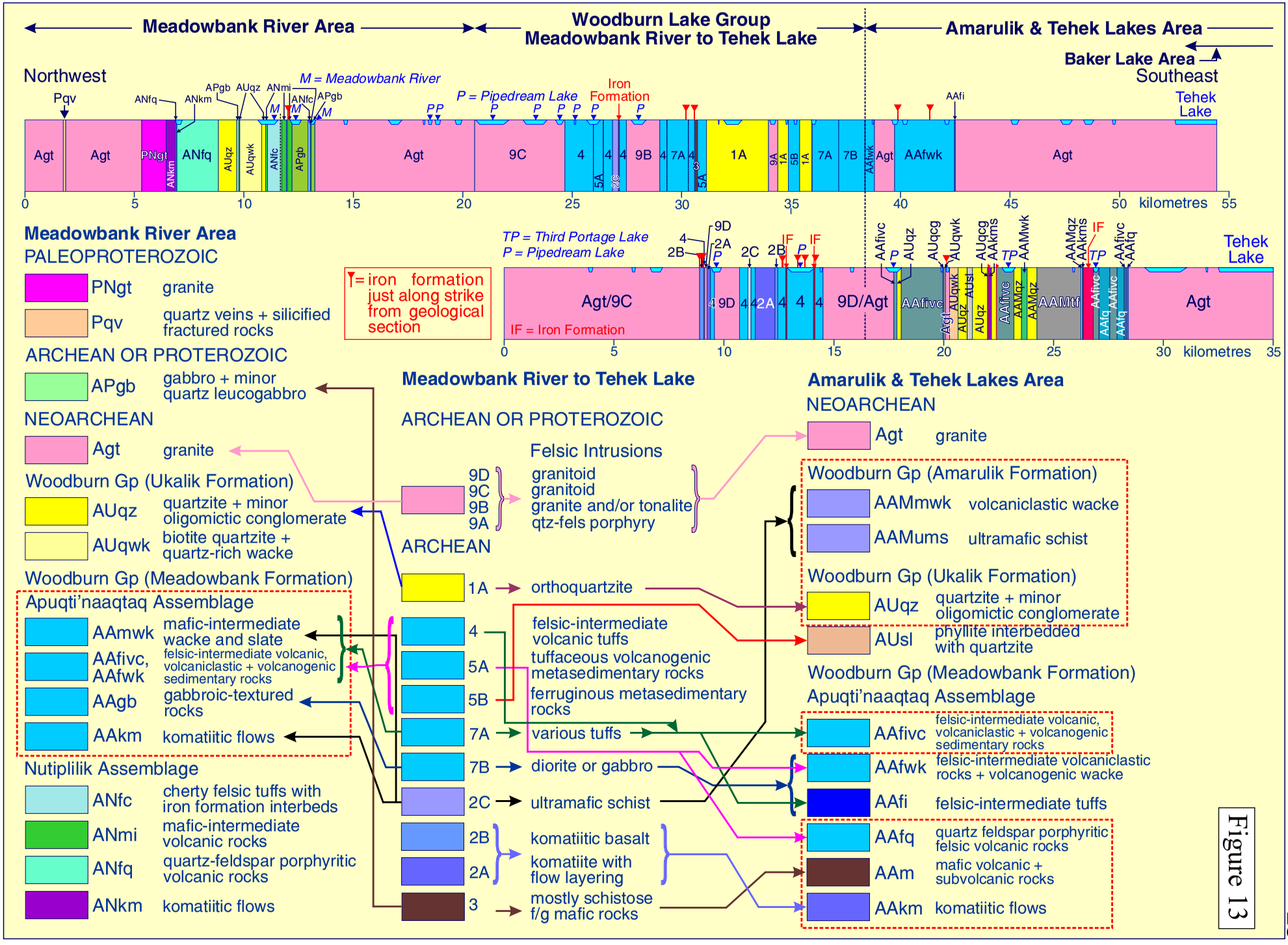
Meadowbank River Area
Woodburn Lake Group
Meadowbank River to Tehek Lake
Amarulik & Tehek Lakes Area
Baker Lake Area
Northwest
Southeast
M = Meadowbank River
P = Pipedream Lake
Iron Formation
Tehek Lake
kilometres
TP = Third Portage Lake
P = Pipedream Lake
IF = Iron Formation
Meadowbank River Area
PALEOPROTEROZOIC
PNgt granite
Pqv quartz veins + silicified fractured rocks
ARCHEAN OR PROTEROZOIC
APgb gabbro + minor quartz leucogabbro
NEOARCHEAN
Agt granite
Woodburn Gp (Ukalik Formation)
AUqz quartzite + minor oligomictic conglomerate
AUqwk biotite quartzite + quartz-rich wacke
Woodburn Gp (Meadowbank Formation)
Apuqti'naaqtaq Assemblage
AAmwk mafic-intermediate wacke and slate
AAfivc, AAfwk felsic-intermediate volcanic, volcaniclastic + volcanogenic sedimentary rocks
AAgb gabbroic-textured rocks
AAkm komatiitic flows
Nutiplilik Assemblage
ANfc cherty felsic tuffs with iron formation interbeds
ANmi mafic-intermediate volcanic rocks
ANfq quartz-feldspar porphyritic volcanic rocks
ANkm komatiitic flows
= iron formation just along strike from geological section
Meadowbank River to Tehek Lake
ARCHEAN OR PROTEROZOIC
Felsic Intrusions
9D 9C 9B 9A granitoid granitoid granite and/or tonalite qtz-fels porphyry
ARCHEAN
1A orthoquartzite
4 felsic-intermediate volcanic tuffs
5A tuffaceous volcanogenic metasedimentary rocks
5B ferruginous metasedimentary rocks
7A various tuffs
7B diorite or gabbro
2C ultramafic schist
2B 2A komatiitic basalt komatiite with flow layering
3 mostly schistose f/g mafic rocks
Amarulik & Tehek Lakes Area
NEOARCHEAN
Agt granite
Woodburn Gp (Amarulik Formation)
AAMmwk volcaniclastic wacke
AAMums ultramafic schist
Woodburn Gp (Ukalik Formation)
AUqz quartzite + minor oligomictic conglomerate
AUsl phyllite interbedded with quartzite
Woodburn Gp (Meadowbank Formation)
Apuqti'naaqtaq Assemblage
AAfivc felsic-intermediate volcanic, volcaniclastic + volcanogenic sedimentary rocks
AAfwk felsic-intermediate volcaniclastic rocks + volcanogenic wacke
AAfi felsic-intermediate tuffs
AAfq quartz feldspar porphyritic felsic volcanic rocks
AAm mafic volcanic + subvolcanic rocks
AAkm komatiitic flows

Figure 13

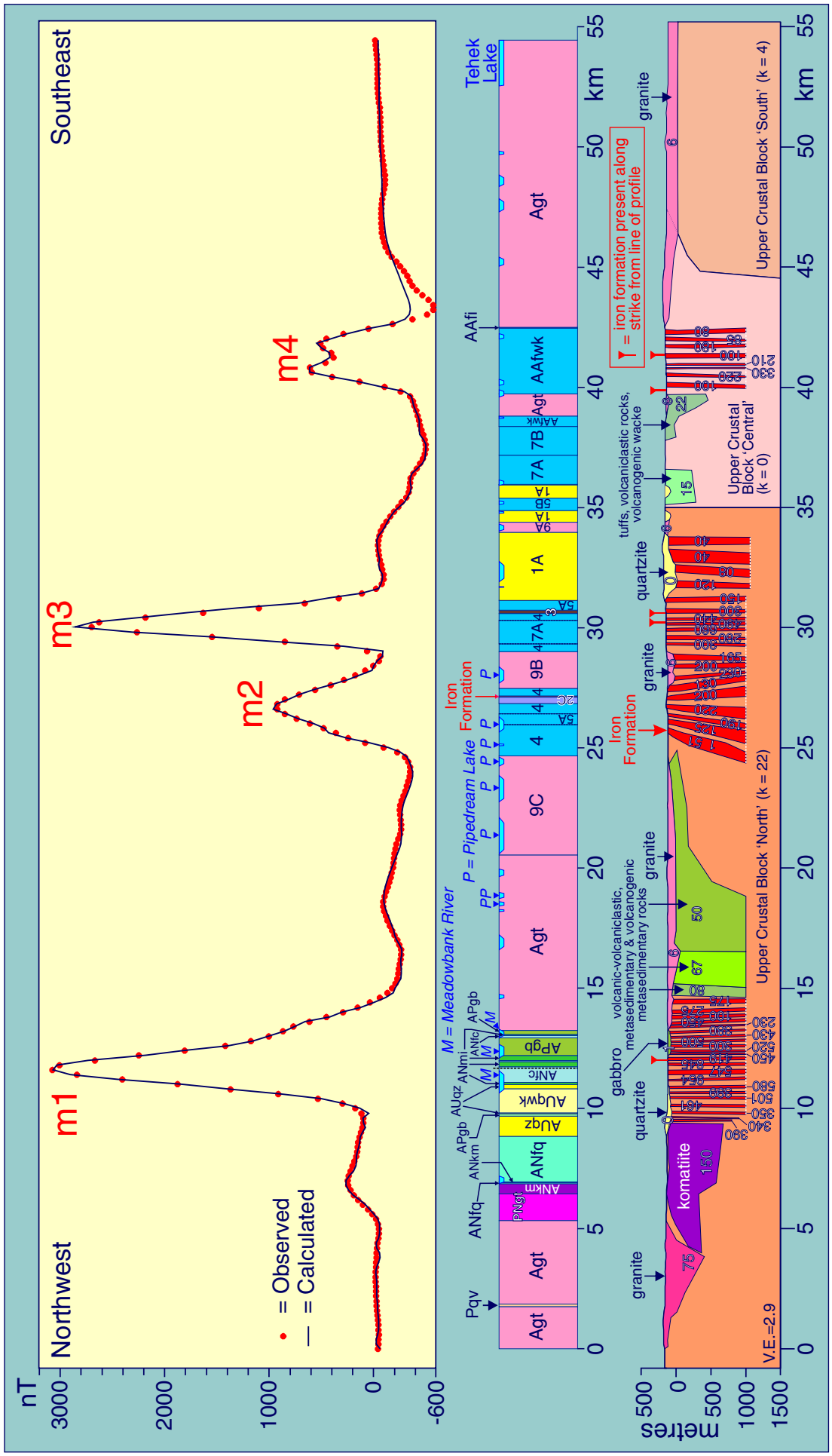

Figure 14: Magnetic model derived from profile along eastern detailed gravity traverse (**A**) together with geological section. Observed and calculated (= modelled) profiles are shown. Legend for section is shown in Figure 13. Numbers within the modelled section represent magnetic susceptibility (k) (x 10^{-3} SI). The principal objective in the first step of modelling was to explain the prominent anomalies (**m1**, **m2**, **m3**, **m4**) by units of iron formation. Secondary magnetic highs and other variations of the magnetic field explained by introduction of volcanic, or volcanic and volcanogenic sedimentary, or granitic units. Each of the three upper crustal blocks extends down to a depth of 5 km below sea level.

A match of the observed magnetic profile along sections where low amplitude magnetic highs are present was attempted by modelling non-iron formation units, while recognizing that susceptibilities of most supracrustal rock types are extremely low (< 1.2 x 10^{-3} SI, Table 1), and that relevant units would have negligible effect on the magnetic field. North of magnetic high **m1** a unit of komatiitic flows (ANkm) that is very narrow at surface has been extended laterally at depth, beneath adjacent granitic rocks to the northwest and porphyritic volcanic rocks (ANfq) and quartzite (AUqz) to the southeast; it descends to almost 700 m below sea level. The unit has a susceptibility of 150 x 10^{-3} SI that is justified by a maximum value of 147 x 10^{-3} SI measured on ultramafic rocks (Table 1). Occurrences (windows?) of komatiitic rocks mapped within unit ANfq and AUqz south of this particular komatiitic unit (Zaleski, 2005) support the modelled extension. North of the komatiitic unit a triangular section of granitic rocks having a large susceptibility value of 75 x 10^{-3} SI is modelled. This value is much larger than measured values for granitic rocks (maximum 15.5 x 10^{-3} SI Table 1). Possibly the triangular unit consists mainly of supracrustal rocks that include komatiitic flows. Much of this portion of the traverse is covered by unconsolidated Quaternary deposits (Zaleski, 2005), and whereas granitic rocks are mapped in a few locations, there is potential for the presence of unmapped supracrustal rocks.

South of magnetic high **m1**, extending almost to **m2**, three units of supracrustal rocks having moderately large susceptibilities (80 x 10^{-3}, 67 x 10^{-3} and 50 x 10^{-3}) have been modelled. The high values are problematical considering the extremely low mean susceptibility values for supracrustal rocks in general (<3.5 x 10^{-3} SI) (Table 1). Even maximum values are not particularly large, with amphibolite attaining 34.2 x 10^{-3} SI and greywacke attaining 26.7 x 10^{-3} SI. Factors contributing to the large modelled values are: (1) values are relative to a fairly high value of 22 x 10^{-3} SI for the Upper Crustal Block "North" required to raise the local background level of the profile; if the bottom of the block was deepened its susceptibility would decrease and comparative susceptibilities for modelled supracrustal units could be lowered, (2) susceptibilities measured on surface outcrop or samples collected from outcrops are influenced by weathering that tends to lower susceptibilities, but to what degree is unknown; possibly this is not a critical factor, but susceptibilities of fresh rock will be larger; (3) the presence of iron formation and/or komatiitic flows and/or dioritic rocks could boost the mean susceptibility of the units.

Two small units of supracrustal rocks have been modelled just north of magnetic high **m4**. Magnetic susceptibilities are 15 x 10^{-3} SI and 22 x 10^{-3} SI, again values larger than expected.

Gravity Model, Traverse A

The Bouguer gravity anomaly map (Fig. 10) is based on a relatively small grid cell size of 1000 m, which helps to maintain some of the detail provided along traverses **A** and **B**. The gravity field is dominated by the regional gravity high **H2** identified in the regional gravity image (Fig. 3) that coincides spatially mainly with supracrustal rocks of the Woodburn Group. The traverses run parallel to and along the southeastern flank of the high between the high **H2** and low **L3** to the southwest. Several relatively short wavelength positive anomalies are evident along the traverses (Fig. 10). These are more clearly defined in the profiles (Figs. 11, 12), having widths ranging from about 1800 m to 7500 m. Magnetic profiles are also plotted in Figures 11 and 12 along with geological sections. Six local gravity highs (**a**, **b**, **c**, **d**, **e**, **f**) occur along Traverse **A** (Fig. 11) and five (**g**, **h**, **i**, **j**, **k**) along Traverse **B** (Fig. 12). In spite of a lack of gravity stations between traverses, continuity between **d** (Traverse **A**) and **h** (Traverse **B**), and between **f** (**A**) and **k** (**B**) is probable. At the south end of both traverses the gravity field decreases relatively rapidly into gravity low **L6** as supracrustal rocks give way to Archean granitic rocks. There is a significant decrease also at the northwestern end of Traverse **A** where supracrustal rocks yield to granitic rocks further north.

The gravity profile along Traverse **A** is dominated by a broad, central gravity high, roughly 40 km wide, attaining a maximum value of about 13 mGal above an estimated lower background gravity field lying at a level of -65.3 mGal (Fig. 11). This high is characterized by the aforementioned short wavelength highs, which have amplitudes relative to an "internal" local background ranging from about 1.7 mGal to 6.7 mGal.

The good correlation of the principal magnetic highs with principal gravity highs (Fig. 11), the definition of iron formations by magnetic modelling and high density of iron formations determined that gravity modelling commence by assigning density values to modelled units of iron formation (Fig. 14). A value of 3.36 g/cm^3, the mean value determined by Symons and Stupavsky (1983) for banded iron formation in the Superior Province, produced a gravity profile (Fig. 15a) containing strong gravity highs displaying generally close spatial coincidence with observed gravity highs **b**, **d, e and f**, but amplitudes of modelled highs are generally noticeably larger. Next, densities converted from magnetic susceptibilities in the magnetic model using the "average equation" of Symons and Stupavsky (1983) were assigned to the iron formations. The match between observed and modelled gravity curves (Fig. 15a) is significantly improved, except in the case of the high **f**. Finally, modelling proceeded empirically, modifying densities until as close a match as possible was achieved between observed and modelled gravity highs in the vicinity of the iron formations (Fig. 15b).

Modelling was completed (Fig. 16) by assigning densities to the non-iron formation units of the magnetic model in Figure 14, and incorporating other geological units as required to reproduce the observed gravity profile. Generally, the original geometries of non-iron formation magnetic model units were either unchanged or only slightly modified.

All short wavelength gravity highs are associated with supracrustal rocks, except for **c**, which falls over granitic rocks. At the northwestern end of the traverse the peak **b** coincides mainly with units APgb (gabbro), ANmi (mafic-intermediate volcanic rocks) and ANfc (cherty felsic tuffs with iron formation interbeds). Table 1 indicates that mean densities of gabbros, intermediate volcanic rocks and mafic volcanic rocks in the area are 3.03 g/cm^3, 2.76 g/cm^3 and 2.89 g/cm^3, respectively. The presence of anomaly **b** over these rock types is compatible with the density data. Iron formation within the tuff unit would also contribute. Gravity high **a** correlates with ANkm (komatiitic flows) and ANfq (quartz-feldspar porphyritic volcanic rocks). Densities of komatiite from the study area are unavailable, but Arndt (1983) indicates a range of 2.77 g/cm^3 (100% serpentinization) to 3.07 g/cm^3 (~10% serpentine) for Archean samples from other areas, and Airo and Mertanen (2008) report densities ranging generally between 2.75 g/cm^3 and 3.00 g/cm^3 for unaltered Palaeoproterozoic komatiites and metaultramafites in the Fennoscandian Shield. Komatiitic rocks, therefore, have potential to contribute to **a** and perhaps to other segments of the **a-b** combined gravity high. Porphyritic volcanic rocks, based on densities of porphyry and felsic volcanic rocks (Table 1), would have a mean density of 2.71 g/cm^3, which is larger than the adopted background density of 2.67 g/cm^3, and could contribute to **a-b**. The minor low between **a** and **b** coincides mainly with AUqz (quartzite) and AUqwk (quartzite and quartz-rich wacke). The relatively low mean density of 2.66 g/cm^3 of quartzite (Table 1) is compatible with a negative signature at this location.

Gravity high **c**, unlike other highs along the traverse, does not correlate with any supracrustal rocks, falling on terrain mapped as Archean or Proterozoic granite, and unlike those highs does not have a prominent corresponding magnetic signature.

Highs **d** and **e** coincide mainly with units of felsic-intermediate volcanic tuffs (unit 4, Fig. 11), tuffaceous volcanic metasedimentary rocks (unit 5A) or various tuffs (unit 7A). These descriptions and descriptions of correlative units (Fig. 13) indicate that such rocks have a bulk composition close to that of an assemblage of felsic-intermediate volcanic rocks, or rocks derived therefrom. Mean densities for felsic and intermediate volcanic rocks (Table 1) are 2.71 g/cm^3 and 2.76 g/cm^3, respectively, producing a positive contrast relative to 2.67 g/cm^3. An intervening low between **d** and **e** correlates partially with a unit of granite (9B).

The gravity high **f** is noticeably asymmetrical, peaking near its southeastern flank, where it coincides with a moderately wide unit (AAfwk) of felsic-intermediate volcaniclastic rocks and volcanogenic wacke. The high decreases gradually northwestward passing over relatively narrow units of granite (Agt) and felsic-intermediate volcaniclastic rocks and volcanogenic wacke (AAfwk), then slightly wider units of diorite or gabbro (7B) and various tuffs (7A), and finally narrow units of orthoquartzite (1A), ferruginous sedimentary rocks (5B), orthoquartzite (1A) and granite (9A). The volcanic and volcanogenic rocks should have similar density attributes to like units associated with gravity highs **d** and **e**, the associated relatively positive density

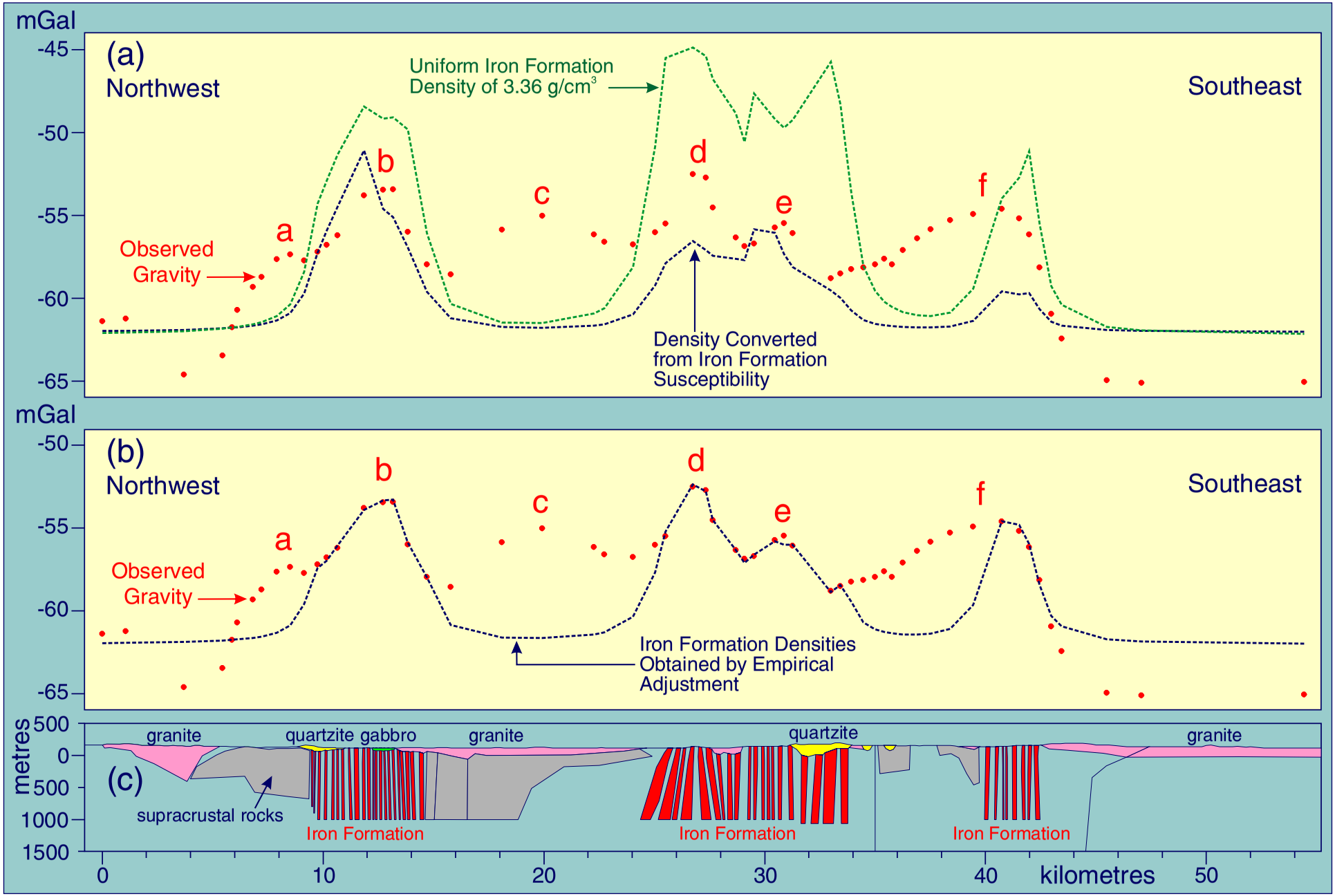

Figure 15: (a) Observed gravity profile along eastern detailed gravity traverse (**A**) and profiles showing gravity effect of iron formation units in the magnetic model of Figure 14, reproduced in (c) based on a uniform density of 3.36 g/m^3 and on densities converted from the model magnetic susceptibilities using the formula of Symons and Stupavsky (1983). (b) Observed gravity profile compared with a profile based on densities empirically modelled to provide a best-fit with the observed profile. (c) magnetic model of Figure 14.

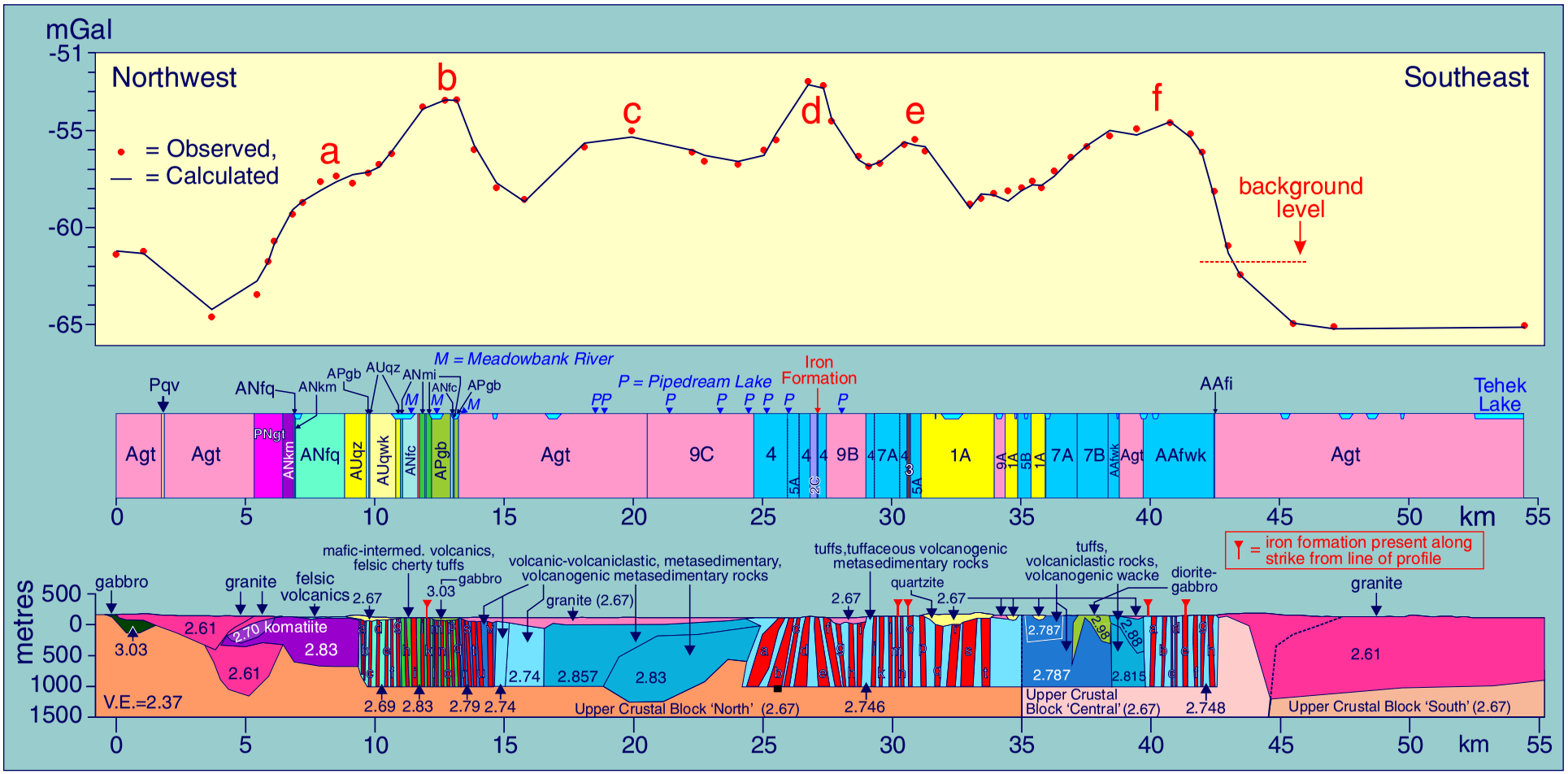

Figure 16: Gravity model derived from profile along eastern detailed gravity traverse (**A**) together with geological section. Observed and calculated (= modelled) profiles are shown. Legend for section is shown in Figure 13. Numbers in the model are densities in g/cm^3. Densities (in g/cm^3) of iron formations (labelled in lower case letters) under gravity highs **a**-**b** are as follows: a, 3.20; b, 3.00; c, 3.0; d, 3.0; e, 2.96; f, 2.92; g, 2.87; h, 3.60; i, 3.122; j, 2.73; k, 2.992; l, 3.191; m, 3.05; n, 2.80; o, 3.00; p, 3.00; q, 3.00; r, 3.05; s, 3.276; t, 2.79; u, 2.72; v, 2.87, under gravity highs **d** and **e** are: a, 2.83; b, 2.79; c, 3.80; d, 2.895; e, 3.24; f, 2.92; g, 2.88; h, 2.90; i, 2.875; j, 2.81; k, 2.82; l, 2.82; m, 2.992; n, 3.00; o, 3.00; p, 2.958; q, 3.00; r, 3.00; s, 2.65; t, 2.85, and under gravity high **f** are: a, 3.36; b, 3.36; c, 3.00; d, 3.20; e, 3.00; f, 3.20; g, 2.87; h, 2.95.

contrast with background granitic rocks being boosted by the presence of the diorite or gabbro unit and probably also by the presence of ferruginous sedimentary rocks.

Notable features of the gravity model from north to south are:

1. A wedge-shaped granite body at the north end of the section defined originally in the magnetic model is assigned a density of 2.61 g/cm^3, typical of Proterozoic granites (Table 1), even though Archean granitic rocks are mapped in this area. It contributes to the gravity low on the north side of gravity high **a**.
2. A contiguous granitic body (2.61 g/cm^3) modelled on the south side of the wedge-shaped unit is also required to help reproduce the low. Its upper portion is a narrow north-dipping sheet, represented by Paleoproterozoic granite at surface, lying above a komatiite body. This sheet connects with a basin-shaped portion of the granite underlying the komatiite unit and descending to about 1300 m below surface.
3. At the northern end of the profile a small gabbroic body (3.03 g/cm^3) is modelled within a heavily drift-covered unit mapped as Neoarchean granite to help restore the modelled profile to background level. Numerous gabbroic bodies invading the granite immediately to the north support its presence.
4. The greater part of a komatiite body modelled under **a** has a density of 2.83 g/cm^3, but its northern, upper portion has a lower density of 2.70 g/cm^3. Notwithstanding the introduction of a granitic body below the northern part of the komatiite, this lighter portion of komatiite is required to improve the match between observed and modelled profiles locally.
5. A broad unit of felsic volcanic rocks (ANfq) mapped beneath gravity high **a** is modelled as a very thin sheet overlying the modelled komatiite unit, from where it extends southeastward under an adjacent quartzitic unit. It thickens abruptly under the quartzitic rocks and continues southeast as far as a unit of mafic-intermediate volcanics (ANmi) underlying the peak and northern flank of gravity high **b**. The rationale for the lateral extension is the widespread presence of ANfq along strike northeast of the quartzitic unit. The modelled felsic unit under the quartzitic rocks terminates at the nominal depth of the bottom of iron formation units about 1000 m below sea level. A density of 2.69 g/cm^3 is assigned to the ANfq unit based on mean densities of 2.67 g/cm^3 and 2.71 g/cm^3 for porphyries and felsic volcanic rocks, respectively.
6. Under much of gravity high **b** a supracrustal unit coinciding with surface units of mafic-intermediate rocks (ANmi), cherty felsic tuffs containing iron formation beds (ANfc) and gabbro (APgb) is modelled, terminating downwards at roughly 1000 m below sea level. It has a density of 2.83 g/cm^3 based on mean densities of 2.76 g/cm^3 and 2.89 g/cm^3 for intermediate and mafic volcanic rocks, respectively (Table 1). The unit of gabbro caps part of the intermediate-mafic volcanic unit (ANmi) and truncates the upper ends of several iron formations. It is believed to be a sill-like intrusion.
7. Between gravity highs **b** and **d** the geology is dominated by mapped Archean or Proterozoic granite, modelled as a thin surficial sheet in the magnetic model (Fig. 14), which is retained in the gravity model (Fig. 16). The northern margin of this sheet coincides with the southern flank of the high **b**, whereas the remainder coincides with the relatively broad high **c**. The latter, unlike other gravity highs along the profile, does not coincide with a magnetic high (Fig. 11), suggesting an absence of significant amounts of iron formation. It does, however, imply the presence of buried supracrustal rocks. Because significant areas of units AAfwk and AAfivc lie along strike northeast of the high, such rocks are probably mainly felsic-intermediate volcanic and volcaniclastic rocks and volcanogenic sedimentary rocks. An appropriate mean density value for such rocks would be 2.74 g/cm^3. Units ANfi (felsic-intermediate volcanic rocks), ANfc (cherty felsic tuffs with iron formation interbeds), and AQwk (greywacke and felsic-intermediate rocks of possible volcanic and volcaniclastic origin) are also present and estimated to have a mean density of 2.74 g/cm^3. Two supracrustal units descending to 1000 m below sea level outlined by the magnetic modelling are retained in the gravity model and assigned densities of 2.74 g/cm^3. These are located in the low between highs **b** and **c**. North of these, under the northern margin of the granite sheet and coinciding with the southern flank of high **b**, a supracrustal unit, density 2.79 g/cm^3, is modelled. The higher density is intermediate between the more general 2.74 g/cm^3 value and the 2.83 g/cm^3 value assumed for a mix of intermediate and mafic volcanic rocks and is based on the presence of unit ANmi (mafic-intermediate volcanic rocks) to the northeast.

Under the southern part of the granite sheet coincident with gravity high **c** a body outlined by magnetic modelling requires a relatively high density of 2.857 g/cm^3 to help reproduce the gravity high, along with the introduction of a body having a density of 2.83 g/cm^3. These densities are compatible with volcanic rocks having compositions ranging from intermediate to mafic. The units descend to about 1000 m and 1250 m below sea level, respectively. A match for gravity high **c** could be obtained using lower densities for these two bodies and a concomitant increase in thickness.

8. Under gravity highs **d** and **e,** where units 4 (felsic-intermediate tuffs), 5A (tuffaceous volcanogenic metasedimentary rocks) and 7A (various tuffs) dominate, a modelled volcanic unit embracing the iron formations and extending to a depth of approximately 1000 m below sea level has a mean density of 2.746 g/cm^3 reflecting a probable felsic-intermediate composition.

9. In the area of gravity high **f** three presumed volcanic units are modelled down to roughly 1000 m below sea level. The southernmost coincides with a surface unit of AAfwk (felsic-intermediate volcaniclastic rocks and volcanogenic wacke). It has a density of 2.748 g/cm^3 consistent with a felsic-intermediate composition. It embraces the units of iron formation in this area. The central unit is segmented into upper and lower parts, coincides in part with a unit of AAfwk and partially underlies a modelled thin sheet of Archean granite. It has a much higher overall density with upper and lower portions having densities of 2.88 g/cm^3 and 2.815 g/cm^3, respectively, suggestive of a predominantly mafic composition. The northern unit has a density of 2.787 g/cm^3 consistent with an intermediate composition, and is partially overlain by a gabbroic unit, density 2.98 g/cm^3, linked to unit 7B (diorite or gabbro) at the surface.

10. A granitic body, density 2.61 g/m^3, is modelled to explain the negative anomaly (L6 on the regional gravity map of Figure 3) at the south end of the profile, spanning the 'Central' and 'South' upper crustal blocks. It has been argued that gravity lows L2 and L3 on the western regional gravity profile (Profile **1**, Fig. 3) were not associated with magnetic patterns indicative of a granitic body at surface, and consequently granitic bodies modelled to explain them were buried (Fig. 8). The granitic body modelled for L6 (Fig. 15) is modelled from the surface downwards, as is the triangular granitic body at the north end of the profile, although distinctive magnetic patterns indicative of a surface presence are not discernible. Notwithstanding the lack of magnetic signatures to support discrete granite bodies at surface, a small Paleoproterozoic syenite-monzodiorite body (maximum dimension ~1800 m) is mapped roughly 10 km southwest of the southeast end of Profile **1** (Zaleski et al., 2005) and the geological map of Paul et al. (2002) shows Proterozoic granite on small islands in Tehek Lake just beyond the southeast end of the profile. This invites speculation that a larger Proterozoic granitic body could be present in the area, if not entirely at surface then mostly buried at shallow depth.

Magnetic Model, Traverse B

The magnetic profile along Traverse **B** contains prominent magnetic highs, and as is the case for Traverse **A** there are good correlations between magnetic and gravity highs along the traverse (Fig. 12). Accordingly, modelling of the magnetic and gravity profiles followed the same approach as used for Traverse **A**.

Three very strong magnetic highs (**m5, m6, m8**), a more moderate high (**m7**) and a weak high (**m9**) are observed along Traverse **B** (Fig. 12). Magnetic high **m6** correlates with **m2** of Traverse **A**, lying on the same linear high. Magnetic high **m7** on Traverse **B** falls near the southwestern end of a linear high represented by **m3** on Traverse **A**, and the high **m8** lies on the same belt of magnetic highs as high **m4** on Traverse **A**.

The magnetic model along Traverse **B** is shown in Figure 17. Modelling commenced by incorporating three upper crustal blocks (bottoms at 5 km below sea level) to reproduce the subtle northwestward increase in the background level of the magnetic field, together with preliminary modelling of the prominent anomalies **m5**, **m6** and **m8** in terms of narrow, steep units of iron formation descending to depths ranging from about 1000 m to 1200 m below the surface. Remaining discrepancies between the observed and modelled profiles were minimised by introducing several magnetic units representing mainly volcanic rocks that attain maximum depths ranging from about 830 m to 1450 m below surface. They are separated by steep contacts. At the

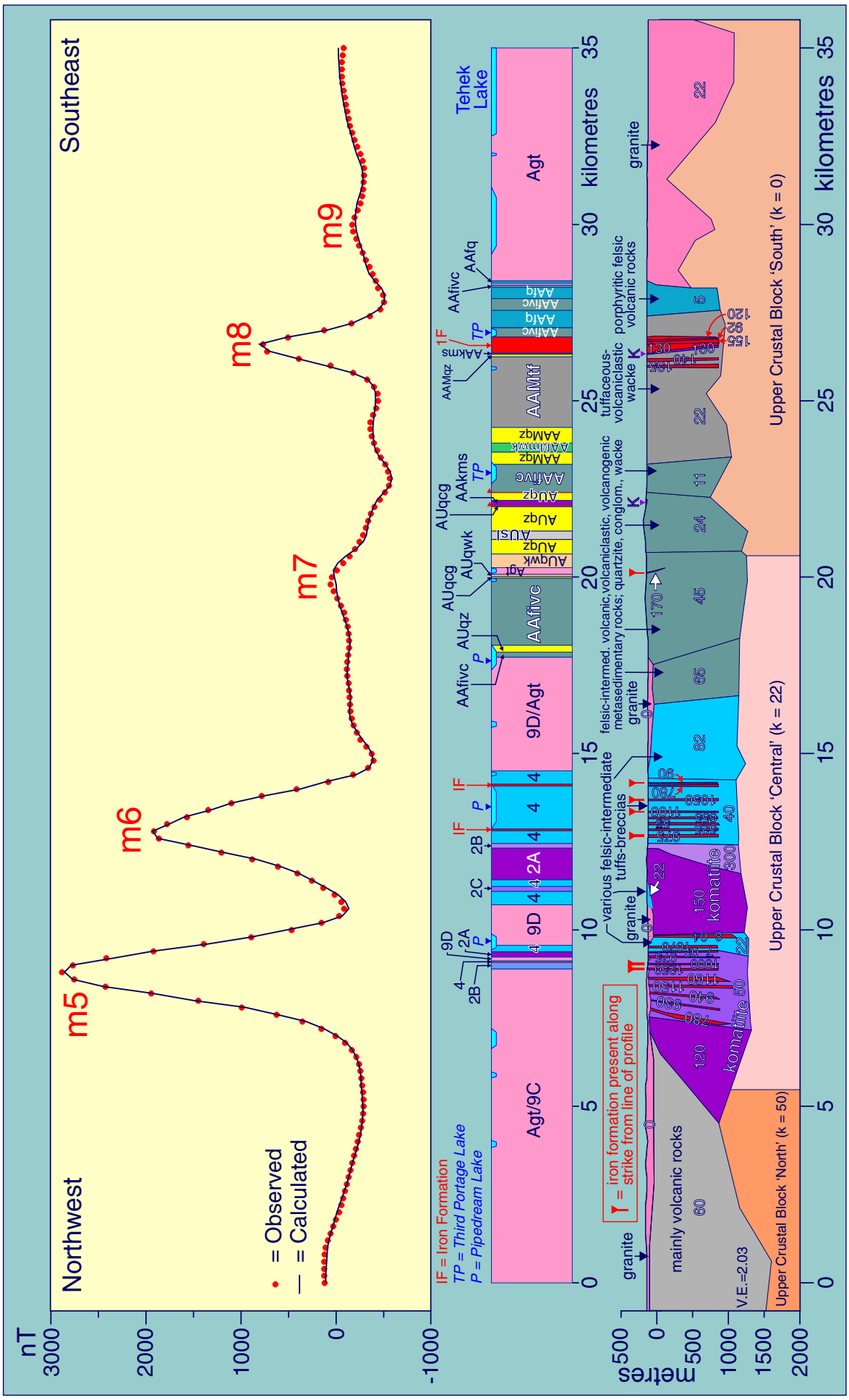

Figure 17: Magnetic model derived from profile along western detailed gravity traverse (**B**) together with geological section. Observed and calculated (= modelled) profiles are shown. Legend for section is shown in Figure 13. Numbers within the modelled section represent magnetic susceptibility (k) (x 10^{-3} SI). Each of the three upper crustal blocks extends down to a depth of 5 km below sea level. K label on modelled section indicates komatiite.

northwest end of the traverse a laterally extensive volcanic unit attains a maximum depth of 1740 m below surface. Magnetic susceptibilities of these units, excluding those of modelled komatiite bodies, range from 5 x 10^{-3} SI to 82 x 10^{-3} SI. Thicknesses of modelled units lying on the 'South' block are marginally smaller than those of units modelled above the 'Central' and 'North' blocks. These patterns may be artufactual, being influenced by the manner in which the regional background is explained by upper crustal blocks having contrasting susceptibilities.

Of particular interest are several bodies of komatiite modelled in the area of magnetic highs **m5** and **m6**. Komatiite units have been mapped at surface but are very much narrower than the units modelled at depth below thin sheets of granite. A case for burial and a wider lateral extent is supported by small granite outliers near Steady Bay that are believed to be in low-angle fault contact with underlying ultramafic rocks (Zaleski et al., 1997). The komatiitic units generally have relatively high susceptibilities compared to those of other supracrustal units, ranging from 120 x 10^{-3} SI to 300 x 10^{-3} SI, though the susceptibility of one unit is as low as 50 x 10^{-3} SI. There is no evidence at surface to support the presence of the large unit of volcanic rocks modelled under a veneer of granitic rocks at the northwest end of the profile, though a requirement for relatively high density rocks at depth in this area is supported by the gravity model (Fig. 18).

At the southeast end of the traverse a granitic body, susceptibility of 22 x 10^{-3} SI, is modelled at surface. Its irregular base is located between 300 m and 1200 m below surface. The northwestern portion of the granite coincides with a minor magnetic high **m9** (Fig. 17) near the south end of a strong magnetic high trending north-northeast that correlates with volcanic and volcanogenic sedimentary rocks containing iron formation north of the granite. Possibly such supracrustal rocks occupy some of the space of the northern part of the granite, though the presence of a negative gravity signature (Fig. 18) indicates that they are not very voluminous.

Gravity Model, Traverse B

The gravity model along Traverse **B** is shown in Figure 18. The model retains the essential geometries of the units defined in the magnetic model (Fig. 17) though several of these units have been subdivided and assigned different densities. There is a good match between the observed and calculated gravity profiles. The principal difference between the magnetic and gravity models is the introduction of a fairly large body of granite at the south end of the model that descends to a depth of roughly 5000 m below the surface. Its presence is required to explain the negative gravity signature of about -6 mGal amplitude relative to a background gravity field level of -61.77 mGal. This amplitude is larger than the -4.9 mGal amplitude determined from the grid used to produce the gravity image in Figure 3, because of smoothing effects when deriving the grid. The granitic body has a density of 2.61 g/cm^3 based on the mean density of only two samples of Proterozoic granite (Table 1). Its uneven upper surface is in contact with a presumed Archean granitic body modelled from the magnetic profile attaining a maximum depth of about 1200 m below surface.

Figure 18 [Next Page]: Gravity model derived from profile along western detailed gravity traverse (**B**) together with geological section. Observed and calculated (= modelled) profiles are shown. Legend for section is shown in Figure 13. Numbers within the modelled section are densities in g/cm^3. Densities (in g/cm^3) of iron formations (labelled in lower case letters) under gravity high **g** are as follows: a, 2.90; b, 2.90; c, 2.85; d, 2.75; e, 2.75; f, 3.10; g, 3.58; h, 3.56; i, 2.82; j, 2.90; k, 2.82, under gravity high **h** are: a, 2.91; b, 2.92; c, 3.10; d, 3.28; e, 3.67; f, 3.10; g, 3.60; h, 3.20, under gravity high **j** is: a, 2.67, and under gravity high **k** are: a, 2.77; b, 2.80; c, 3.10; d, 3.00; e, 2.70; f, 2.77. K label on modelled section indicates komatiite.

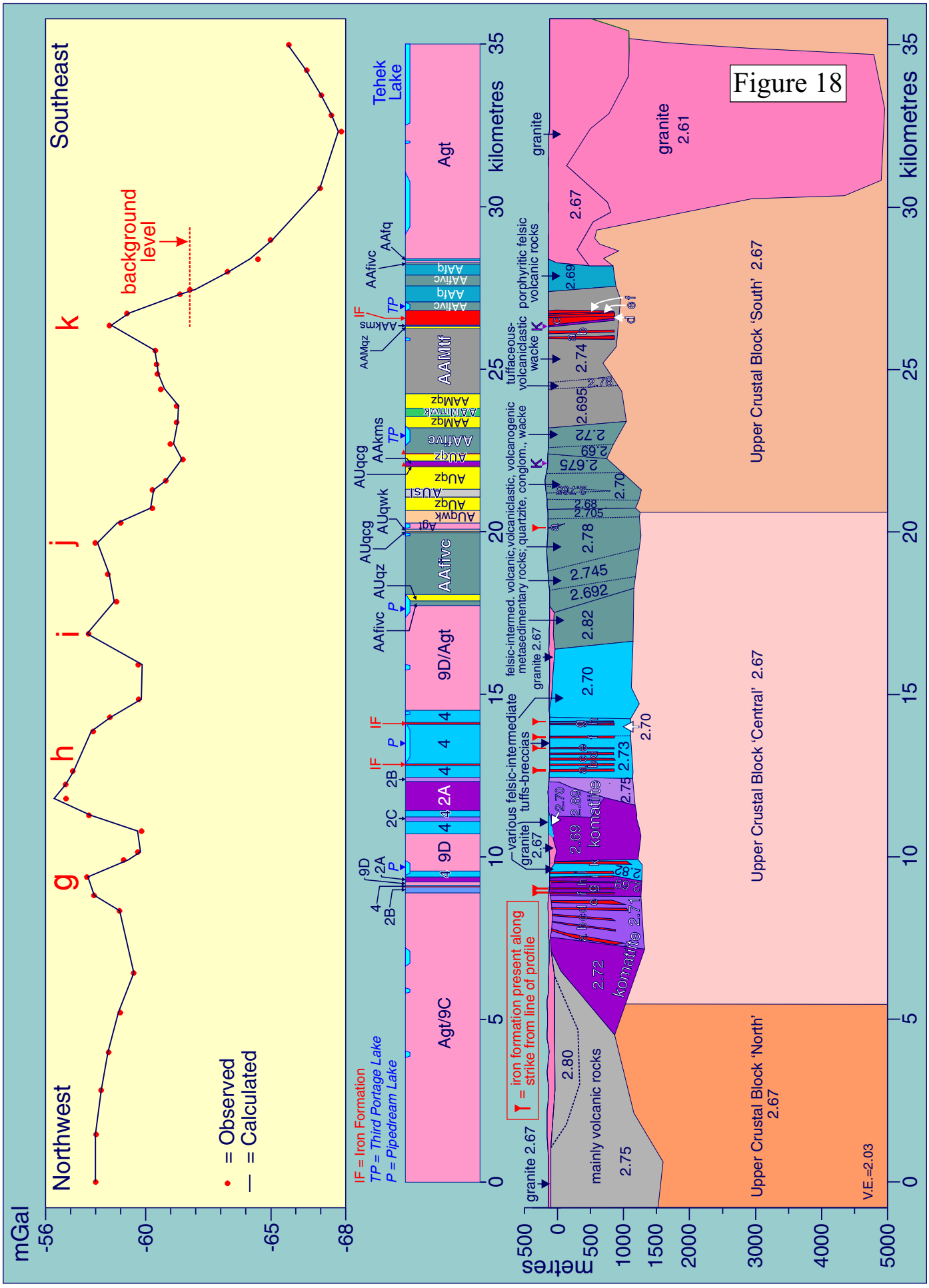
Figure 18
mGal
Northwest
Southeast
g h i j k
background level
= Observed
= Calculated
IF = Iron Formation
TP = Third Portage Lake
P = Pipedream Lake
Tehek Lake
kilometres
metres
granite 2.67
mainly volcanic rocks
2.75
2.80
Upper Crustal Block 'North' 2.67
Upper Crustal Block 'Central' 2.67
Upper Crustal Block 'South' 2.67
granite 2.61
V.E.=2.03

Conclusions

Modelling of gravity and magnetic profiles along the paths of two detailed (relatively closely spaced measurements) gravity traverses has provided a preliminary picture of the shallow crustal geology in the general area of the Meadowbank gold deposits. Supracrustal and granitic units are modelled along both traverses and generally they extend no deeper than 1750 m below the surface, though one granitic body attains a depth of about 5000 m. Because of characteristically relatively small density contrasts between various supracrustal units, and because of the presence of very large magnetic anomalies linked to iron formations, modelling of magnetic data was completed as a first step and magnetic models were then used as a guide for gravity modelling.

The steep and narrow nature of modelled iron formation units resulted in arbitrary termination of the units at a uniform depth of about 1100 m below surface in the model for Traverse **A** (Fig. 16), and generally at about 1000 m ranging up to about 1200 m in the model for Traverse **B** (Fig. 18). Further deepening of such narrow units does not visibly change the modelled profile. The depths of the iron formation units, which are hosted by supracrustal volcanic and/or volcanogenic metasedimentary units, influenced the depths of modelled supracrustal units to maintain some consistency in the vertical distribution of iron formations and hosts, at the same time using reasonable densities. With few exceptions, contacts between supracrustal units are steep. The large volume of iron formation is one of the most interesting results of the study, given their limited mapped distribution.

A noteworthy feature of the models along both traverses is a requirement for much larger volumes of komatiite near their north ends. An implication in the case of Traverse **B** is a possible thrust contact between komatiite and two modelled thin sheets of overlying granitic rocks. Evidence for such a contact just a few kilometres south of the traverse has been noted (Zaleski et al., 1997).

A consequence of a regional background gravity field at a level of -61.77 mGal is a negative gravity signature at the south end of Traverse **A,** and north and south ends of Traverse **B**. In the models these are attributed to lower density (2.61 g/cm^3) Proterozoic granite bodies (Figs. 16, 18). The proposed granite body at the south end of Traverse **B** has a vertical extent of about 5000 m.

An arbitrary aspect of the models along the traverses is the requirement for sub-supracrustal upper crustal blocks having bases at a depth of 5000 m below sea level and different magnetic susceptibilities. These blocks provide one means of reproducing a regional northwestward increase in the magnetic field. A consequence of the moderately high susceptibilities required for the blocks is that even higher susceptibilities must be applied to several supracrustal units to produce sufficiently large contrasts between the units and crustal blocks to satisfy the observed magnetic profile. The supracrustal susceptibilities are significantly larger than measured susceptibilities. Possible reasons have been advanced to explain this discrepancy, but it remains a disconcerting aspect of the models.

The relatively small thicknesses, generally 500 m to 1700 m, of supracrustal rocks modelled along Traverse **A** and **B** accord well with thicknesses, generally 1000 m to 2000 m, modelled along significant sections of the regional gravity profiles **1** and **2**, though local keels attain 2.8 km, 4.6 km and 8.3 km. The regional gravity model along Profile **2** indicates that Archean granitic rocks are present as thin sheets above supracrustal rocks. The nature of their contacts is debatable as both tectonic and intrusive contacts have been reported in the study area. Small, yet distinct, gravity lows in the regional gravity field have been modelled as relatively thin (~ 3 km thick) buried granitic bodies regarded to be Proterozoic.

The presented models are essentially unconstrained, other than by a relatively small data base of densities and magnetic susceptibilities measured on samples scattered thinly throughout the area. A section of a magnetotelluric transect (Jones et al., 2002) roughly parallel to regional gravity Profile **2** (transect stations 6, 7 and 8 are plotted in Figure 2) does not have the required resolution to assist gravity or magnetic modelling. The gravity and magnetic models are not unique, but present a viable picture of the shallow crust along the detailed transects that can be used as a guide for further investigations. Given the complex, multiphase structural history of the region the steep and parallel attitudes of the many modelled iron formations are questionable, as are the

steep attitudes of most contacts between supracrustal units. The actual structural picture may differ in detail, but large volumes of iron formation are required to reproduce the observed magnetic signatures and steep contacts facilitated the modelling process. Better rock property data and other independent constraints would help refine these preliminary models.

Acknowledgements

I wish to thank several colleagues and former colleagues for various forms of assistance and information. Charlie Jefferson, Leader, GEM Uranium Project for continued support and enthusiastic encouragement, and Leslie Chorlton, John Kerswill, Deborah Lemkow, Sally Pehrsson and Lori Wilkinson for geological information and data. I am also most grateful to Charlie Jefferson for a critical review of this report and constructive comments.

References

Airo, M. L. and Mertanen, S. 2008. Magnetic signatures related to orogenic gold mineralization, Central Lapland Greenstone Belt, Finland. Journal of Applied Geophysics, 64, 14-24.

Arndt, N.T. 1983. Role of a thin komatiite-rich oceanic crust in the Archean plate-tectonic process. Geology, 11, 372-375.

Ashton, K.E. 1987. Southeastern Amer Lake Area (66H/1), District of Keewatin, Northwest Territories. Geological Survey of Canada, Open File 1685, Scale 1:50,000.

Ashton, K.E. 1988. Precambrian Geology of the Southeastern Amer Lake area (66H/1), near Baker Lake, N.W.T. Ph.D. Thesis, Queen's University, Kingston, Ontario, Canada.

Fraser, J.A. 1987. Geology, Woodburn Lake, District of Keewatin, Northwest Territories. Geological Survey of Canada, Map 1656A, Scale 1: 250 000.

Goodge, J.W. and Finn, C.A. 2010. Glimpses of East Antarctica: Aeromagnetic and satellite magnetic view from the central Transantarctic Mountains of East Antarctica. Journal of Geophysical Research, 115, B09103, 22 p., doi:10.1029/2009JB006890.

Henderson, J.R. and Henderson, M.N. 1994. Geology of the Whitehills Tehek Lakes area, District of Keewatin, Northwest Territories. Geological Survey of Canada, Open File 2923, Scale: 1:100 000.

Jones, A.G., Snyder, D., Hanmer, S., Asudeh, I. and White, D. 2002. Magnetotelluric and teleseismic study across the Snowbird Tectonic Zone, Canadian Shield: A Neoarchean mantle structure? Geophysical Research Letters, 29, 1829, doi:10.1029/2002GL015359.

Paul, D., Hanmer, S., Tella, S., Peterson, T.D. and LeCheminant, A.N. 2002. Geology, compilation, bedrock geology of part of the Western Churchill Province, Nunavut-Northwest Territories. Geological Survey of Canada, Open File 4236, scale 1:1 000 000.

Peterson, T.D. 2006. Geology of the Dubawnt Lake area, Nunavut-Northwest Territories. Geological Survey of Canada, Bulletin 580, 56 p.

Schau, M. 1983. Baker Lake. Geological Survey of Canada, Open File 883 (Geological Map and Marginal Notes), Scale 1:125 000.

Sherlock, R., Pehrsson, S., Logan, A.V., Hrabi, R.B. and Davis, W.J. 2004. Geological setting of the Meadowbank gold deposits, Woodburn Lake Group, Nunavut. Exploration and Mining Geology, 13, 67-107.

Symons, D.T.A. and Stupavsky, M. 1983. Part I: Component magnetization of Algoman banded iron formations and deposits in Ontario. Ontario Geological Survey, Open File Report 5447, 2-18.

Tella, S. 1994. Geology, Amer Lake (66H), Deep Rose Lake (66G), and parts of Pelly Lake (66F), District of Keewatin, Northwest Territories. Geological Survey of Canada, Open File 2969, Scale 1:250 000.

Tompkins, L.A. and Cowan, D.R. 2001. Opaque mineralogy and magnetic properties of selected banded iron-formations, Hamersley Basin, Western Australia. Australian Journal of Earth Sciences, 48, 427-437.

Zaleski, E. 2005. Geology, Meadowbank River area, Nunavut. Geological Survey of Canada, Map 2068A, Scale 1:50 000.

Zaleski, E. and Pehrsson, S. 2005. Geology, Half Way Hills and Whitehills Lake area, Nunavut. Geological Survey of Canada, Map 2069A, Scale 1:50 000.

Zaleski, E, Pehrsson, S. and Wilkinson, L. 2005. Geology, Amarulik and Tehek lakes area, Nunavut. Geological Survey of Canada, Map 2070A, Scale 1:50 000.

Zaleski, E., Corrigan, D., Kjarsgaard, B.A., Kerswill, J.A., Jenner, G.A. and Henderson. J.R. 1997. Geology, Woodburn Lake Group, Meadowbank River to Tehek Lake (66H/1, 56E/4), District of Keewatin (Nunavut), Northwest Territories. Geological Survey of Canada, Open File 3461, Scale 1:50 000.

Zaleski, E., Pehrsson, S., Duke, N., Davis, W. J., L'Heureux, R., Greiner, E., and Kerswill, J. A., 2000. Quartzite sequences and their relationships, Woodburn Lake group, western Churchill Province, Nunavut. Geological Survey of Canada, Current Research 2000-C7, 10 p.